X-621-73-35

PREPRINT

NASA TM X- 66189

FULL NON-LINEAR TREATMENT OF THE GLOBAL THERMOSPHERIC WIND SYSTEM

PART 1: MATHEMATICAL METHOD AND ANALYSIS OF FORCES

P. W. BLUM
I. HARRIS

JANUARY 1973

GSFC — GODDARD SPACE FLIGHT CENTER

GREENBELT, MD.

FULL NON-LINEAR TREATMENT OF THE GLOBAL THERMOSPHERIC WIND SYSTEM. PART 1: MATHEMATICAL METHOD AND ANALYSIS OF FORCES

P. W. Blum* and I. Harris

January 1973

*NRC/NAS Research Associate

Goddard Space Flight Center

Greenbelt, Maryland

CONTENTS

ABSTRACT

The equations of horizontal motion of the neutral atmosphere between 120 and 500 km are integrated with the inclusion of all the non-linear terms of the convective derivative and the viscous forces due to vertical and horizontal velocity gradients. Empirical models of the distribution of neutral and charged particles are assumed to be known. The model of velocities developed is a steady state model. In part 1 the mathematical method used in the integration of the Navier-Stokes equations is described and the various forces are analysed.

FULL NON-LINEAR TREATMENT OF THE GLOBAL THERMOSPHERIC WIND SYSTEM.

Introduction

The wind system of the thermosphere has been a subject of a considerable number of observational and theoretical investigations during the last decade. A knowledge of this wind system is required for an understanding of the structure of the neutral atmosphere and its energy balance and the ionosphere. It has been suggested that the solution of the phase problem (the phases of the density and temperature in the thermosphere) of the neutral atmosphere is intimately connected with the wind system. Many ionospheric effects concerning the latitudinal distribution of charged particles, the daily variation of electron density and the maintenance of the nighttime ionosphere cannot be fully explained without taking into account the effect of the atmospheric wind system.

Several computations of the thermospheric wind pattern have been made. All of them solve the horizontal equations of motion and assume hydrostatic equilibrium. There are two general approaches: (1) a perturbation treatment of the full set of hydrodynamic equations (Lindzen (1970); Volland and Mayr (1970 and 1972); (2) a solution of the equation of motion using a given model of atmospheric structure (Geisler (1967); Bailey et al. (1969); Challinor (1970); Cho and Yeh (1970); Rüester and Dudeney, (1972)). The various computations

differ in the assumptions regarding the treatment of the ion and viscous drag. All of them have in common that the non-linear terms of the convective derivative of the flow velocity were not fully included. Especially the non-linear terms due to meridional velocity gradients have not been included in the computation by any of the investigators.

We have chosen the second approach, i.e., we have used in our calculations the atmospheric model of Jacchia (1965) and the Penn State Ionospheric Model of Nisbet (1970) and solved the full Navier-Stokes equations including all non-linear terms and the full expression for the viscous forces. None of the earlier papers have included in the computations of the viscous terms the horizontal velocity gradients.

1. MATHEMATICAL METHOD

The Steady State

The neutral air motions treated here are steady state motions. The steady state refers to the sun's system. All variables like density, temperature, velocities and the various forces are assumed to be independent of universal time in a coordinate system fixed with respect to the sun, if we limit ourselves to periods of a few days. Variations with universal time due to the changing declination of the sun, solar activity or the semi-annual density variation are not excluded, but each change of this type is treated as a separate model calculation. Therefore for each day of the year and a given solar activity our set of equations has

three independent variables. For these we have chosen the height z, i.e. the distance from the surface of the earth, the geographical co-latitude θ and the azimuth ϕ referred to a coordinate system not rotating with the earth. ϕ is identical with the local time τ. These simplifying assumptions exclude the treatment of physical processes that have a true universal (not local) time dependence with time scales of a day or less. Such processes would include all effects that are due to the inclination between the earth's axis and its magnetic dipole. In the reference frame that rotates with the earth the independence from universal time means that all variables depend only upon the combination $\lambda - \omega t$ of geographical longitude λ and universal time t, i.e. all phenomena are periodic with the period $2\pi/\omega$ of one solar day. Non-recurring changes, sporadic variations and variations that depend explicitly on longitude λ and not only on $\tau = \lambda - \omega t$ are excluded from our treatment.

To obtain the appropriate form of the hydrodynamic equations for an observer on the earth, we must first transform the equations to a frame rotating with the earth and then take the limit to the steady state. Let ϕ be the longitude in the fixed frame and λ the longitude in the rotating frame, and let t' be the time in the rotating frame and t in the fixed frame. Then the transformation equations are

$$\lambda = \phi - \omega t \tag{1}$$

$$t' = t$$

The partial derivative with respect to ϕ and t are according to the chain rule

$$\frac{\partial}{\partial \phi} = \frac{\partial}{\partial \lambda}$$

$$\frac{\partial}{\partial t} = \frac{\partial}{\partial t'} - \omega \frac{\partial}{\partial \lambda} \tag{2}$$

In the steady state we can let the partial derivative with respect to the time t in the fixed frame go to zero and thus obtain the following relationship between the time variations and the longitude variations for an observer on the earth

$$\frac{\partial}{\partial t'} = \omega \frac{\partial}{\partial \lambda} \tag{3}$$

Care must be exercised when this relationship is used; in particular one must not try to describe transient phenomena using equations based upon these relationships. Boundary conditions imposed upon the equations must be consistent with the assumption of the steady state.

It is to be noted that the solutions of the tidal equations (Chapman and Lindzen, (1970)) that would correspond to the steady state are those for which the parameters f and s (in their notation) of tidal theory have the ratio unity.

Equations of Motion

The Navier-Stokes equations in vector form in the rotating frame are

$$\frac{D\vec{V}}{Dt} + 2\vec{\omega} \times \vec{V} - \eta \operatorname{div} \operatorname{grad} \vec{V} - \eta/3 \operatorname{grad} \operatorname{div} \vec{V} + \vec{f}_{ion} = -(\operatorname{grad} P)/\rho + \vec{g} \tag{4}$$

where $\vec{V}$ is the velocity vector, $\vec{\omega}$ the rotational velocity of the earth, $\vec{f}_{ion}$ the ion drag force, P the pressure, ρ the density and η the kinematic viscosity.

We are concerned with the global wind pattern with periods of the order of one day and its harmonics. The appropriate coordinate system for this problem

is spherical. As the vertical velocities are smaller by more than one order of magnitude than the horizontal velocities, we may solve the horizontal equations neglecting the vertical velocity terms that appear in the convective derivative, the Coriolis force and the viscous forces.

Let $V^{(\theta)}$ be the meridional velocity, measured positive from North to South, and $V^{(\phi)}$ the zonal velocity, measured positive from West to East, then the convective derivative of the velocities becomes

$$\frac{DV^{(\theta)}}{Dt} = \omega \frac{\partial V^{(\theta)}}{\partial \phi} + \frac{1}{r}\left(V^{(\theta)} \frac{\partial V^{(\theta)}}{\partial \theta} + \frac{V^{(\phi)}}{\sin\theta} \frac{\partial V^{(\theta)}}{\partial \phi} (V^{(\phi)})^2 \operatorname{ctn} \theta\right)$$

$$\frac{DV^{(\phi)}}{Dt} = \omega \frac{\partial V^{(\phi)}}{\partial \phi} + \frac{1}{r}\left(V^{(\theta)} \frac{\partial V^{(\phi)}}{\partial \theta} + \frac{V^{(\phi)}}{\sin\theta} \frac{\partial V^{(\phi)}}{\partial \phi} + V^{(\theta)} V^{(\phi)} \operatorname{ctn} \theta\right) \quad (5)$$

with θ the co-latitude and ϕ the longitude in the sun's system (or local time in the earth's system) and r the distance from the center of the earth.

We have made use in these equations of the steady-state assumptions, i. e., we have assumed all variables to depend only upon local time and not explicitly upon geographic longitude and universal time.

Substituting the expressions for the convective derivatives in the Navier-Stokes equations and dividing by ω, it is seen that the non-linear terms are multiplied by a factor $1/(\omega r)$. The numerical value of ωr is 462 m/sec. The main inertial term $\partial \vec{V}/\partial \phi$ is of the order of the velocity itself. Without detailed calculations this suggests that for velocities that are lower by an order of

magnitude than ωr it is to be expected that the non-linear terms have no marked influence on the results. On the other hand for velocities that are comparable or larger than ωr it is essential to include the non-linear terms. This estimate is based on the assumption that the derivatives of the velocities are of the order of the velocities themselves (in the spherical coordinate system) which is obviously true for the zonal derivatives, but may not be true, and indeed is not in the equatorial region, for the meridional gradients.

The equations we now have to solve are a pair of non-linear coupled second order partial differential equations with the three independent variables r, θ and ϕ or r, θ and τ. According to the steady state picture the solutions must be periodic in local time (the variable τ), finite and continuous everywhere. The boundary conditions in altitude specify a given distribution of velocities at the lower boundary and a zero vertical gradient of horizontal velocities at the upper boundary. Not every density model and ion distribution would result in a steady state solution. This is seen by the simple considerations that pressure gradients that are too large cannot be maintained due to the rapid flow which would tend to equalize these pressure gradients. We shall assume that a solution exists based upon empirical models of the atmosphere and ion distribution. From the assumption of the existence of the solution certain limitations of the velocity distribution may be obtained. At equinox conditions, where from symmetry considerations the meridional component of velocity is zero at the equator, the equation for the zonal component of velocity becomes

$$\left(1 + \frac{V}{\omega r}\right) \frac{\partial V}{\partial \tau} = - \frac{1}{\omega r \rho} \frac{\partial p}{\partial \tau} - D(\tau) V + \eta(\tau) \frac{\partial^2 V}{\partial r^2} \qquad (6)$$

where D is the ion drag coefficient for unit mass.

A theorem by Kallina (1970) states that a sufficient condition for the existence of a periodic solution of equation (6) is that the coefficient $(1 + V/\omega r)$ of $\partial V/\partial \tau$ is positive for all τ and r. Thus, in this simple case, we may expect a periodic solution with the model pressure gradients and ion drag coefficients as long as the zonal velocity in the westward direction remains less than the earth's rotational velocity. However, if the zonal velocity exceeds the rotational velocity of the earth in the westward direction then one would expect to obtain exponential growing solutions and no periodic or steady state solution. A steady state solution for such a model of the atmosphere and ionosphere would not exist. If at any stage in the computational process one obtains zonal velocities of this behaviour numerical instabilities will develop. For example, if the values of the driving force divided by ω would be used as initial values for V in an iterative procedure for the solution of the steady state horizontal flow equations, then with the model pressure gradients of the Jacchia model the numerical solution would diverge. Kallina's theorem needs to be generalized in order to guide us concerning the existence of a solution for the full set of equations (4) for the horizontal flow under general conditions. Such a generalization is at present not available.

In a purely linear treatment this property of the velocity field would not be apparent. Any model of atmospheric density and ion distribution results in a steady state velocity field when the non-linear terms of the convective derivative are neglected. Only the full non-linear treatment shows that the steady state does not exist if certain conditions are not met, i. e. the ratio of the driving forces to the drag forces is too large. It may be argued that Kallina's theorem does not unequivocally show this property of the velocity field, as it treats only a very simplified system of equations and furthermore gives only sufficient and not necessary conditions for the existence of a steady state solution. On the other hand we have made a large number of numerical model calculation that indicated that a generalization of Kallina's theorem must be true. These model calculations converged always when a parameter R, which indicated the ratio between driving and drag forces, was smaller than a certain R_0. They diverged for all models with R greater than R_0, thus indicating that steady state solutions for such models do not exist. The value of R_0 was well defined, a very small excess of R over R_0 caused the models to diverge immediately.

Method of Solution

The condition of periodicity will be satisfied if we expand each term of equation (4) into Fourier modes with respect to local time. The velocity is decomposed into average (or zero order), diurnal and semi-diurnal harmonic components; each component is taken as a function of latitude and altitude.

Also the pressure gradients divided by density, the kinematic viscosity and the ion drag coefficient are expressed in a similar fashion. Accordingly the velocities will be expressed by

$$V^{(\theta)}(\phi, \theta, r) = \sum_{k=0}^{2} \left(a_k^{(\theta)}(\theta, r) \cos 2\pi k\phi + b_k^{(\theta)}(\theta, r) \sin 2\pi k\phi\right)$$

$$V^{(\phi)}(\phi, \theta, r) = \sum_{k=0}^{2} \left(a_k^{(\phi)}(\theta, r) \cos 2\pi k\phi + b_k^{(\phi)}(\theta, r) \sin 2\pi k\phi\right) \tag{7}$$

All products of Fourier terms which give rise to modes higher than the semi-diurnal mode are dropped in the calculations. Thereby we have reduced the problem to the solution of ten coupled non-linear partial differential equations of second order for the ten unknown functions a_k and b_k (with $b_0 = 0$) with altitude and latitude as the independent variables. A finite difference scheme is used to obtain the solutions. The derivatives with respect to latitude are replaced by second order differences, except at the north and south poles, where forward and backward differences are used respectively. The first derivative with respect to altitude is not present in our equations. The second derivatives with respect to altitude are replaced by normal second order differences. The boundary conditions in altitude are expressed to second order accuracy (Varga, p. 191).

Treatment of the Equations at the Poles

Previous investigations of the global wind field have either excluded the polar regions of have used a simplified computational scheme (sometimes using Cartesian coordinates). This can be done without great loss of accuracy if the latitudinal coupling of the wind field is neglected. In our treatment such simplifications are not possible. The inclusion of the poles in the computational scheme requires some care and we therefore present some details of our approach.

The boundary condition that the solution be single valued at the poles requires that all modes of the horizontal velocity but the diurnal mode vanish at the poles as can be seen by simple kinematical considerations. Furthermore, the meridional and the zonal components of velocity are ninety degrees out of phase. Thus we must have

$$\begin{aligned} a_1^{(\phi)} &= b_1^{(\theta)} \cdot \text{sig} \\ b_1^{(\phi)} &= -a_1^{(\theta)} \cdot \text{sig} \end{aligned} \tag{8}$$

where sig = +1 at the north pole and -1 at the south pole. Also we have

$$a_k^{(\theta)} = b_k^{(\theta)} = a_k^{(\phi)} = b_k^{(\phi)} = 0 \tag{9}$$

for k not equal to one. These kinematical boundary conditions at the poles reduce the number of unknown velocity components at each pole from ten to two.

On the other hand the system of equations (4) yields four separate equations (two for each of the diurnal modes for both the meridional and the zonal components), so the problem seems to be overdetermined at the poles.

Formally at the poles the Navier-Stokes equations appear to have a singularity due to the factor $(1/\sin\theta)$ that appears in some of the non-linear terms. Let $L^{(\theta)}$ and $L^{(\phi)}$ be those terms then

$$L^{(\theta)} = \frac{V^{(\phi)}}{\sin\theta}\left[\frac{\partial V^{(\theta)}}{\partial\phi} - V^{(\phi)}\cos\theta\right]$$

$$L^{(\phi)} = \frac{V^{(\phi)}}{\sin\theta}\left[\frac{\partial V^{(\phi)}}{\partial\phi} + V^{(\theta)}\cos\theta\right] \qquad (10)$$

But from boundary conditions (8) and (9) it is seen that the bracketed parts of $L^{(\theta)}$ and $L^{(\phi)}$ vanish at the poles and $L^{(\theta)}$ and $L^{(\phi)}$ become therefore indeterminate. To evaluate this indeterminate form of the non-linear terms we have to apply L'Hospital's rule at the poles. The expressions (10) become

$$L^{(\theta)} = \frac{V^{(\phi)}}{\cos\theta}\left[\frac{\partial^2 V^{(\theta)}}{\partial\theta\,\partial\phi} - \cos\theta\,\frac{\partial V^{(\phi)}}{\partial\theta}\right]$$

$$L^{(\phi)} = \frac{V^{(\phi)}}{\cos\theta}\left[\frac{\partial^2 V^{(\phi)}}{\partial\theta\,\partial\phi} + \cos\theta\,\frac{\partial V^{(\theta)}}{\partial\theta}\right] \qquad (11)$$

We have to evaluate $L^{(\theta)}$ and $L^{(\phi)}$ for the diurnal modes only, as we have already shown that the other modes vanish at the poles. It is easily seen that the product $V^{(\phi)}\ \partial^2 V/\partial\theta\,\partial\phi$ is zero also for the diurnal modes. Therefore at the poles the expressions (11) are reduced to

$$L^{(\theta)} = -V^{(\phi)}\frac{\partial V^{(\phi)}}{\partial\theta}$$

$$L^{(\phi)} = V^{(\phi)}\frac{\partial V^{(\theta)}}{\partial\theta} \qquad (12)$$

Substituting (12) into the full expression of the convective derivative as given by equations (5) we obtain

$$\frac{DV_1^{(\theta)}}{Dt} = \omega\frac{\partial V_1^{(\theta)}}{\partial\phi} + \frac{1}{r}\left(V^{(\theta)}\frac{\partial V^{(\theta)}}{\partial\theta} - V^{(\phi)}\frac{\partial V^{(\phi)}}{\partial\theta}\right)_1$$

$$\frac{DV_1^{(\phi)}}{Dt} = \omega\frac{\partial V_1^{(\phi)}}{\partial\phi} + \frac{1}{r}\left(V^{(\phi)}\frac{\partial V^{(\phi)}}{\partial\theta} + V^{(\phi)}\frac{\partial V^{(\theta)}}{\partial\theta}\right)_1 \qquad (13)$$

The subscript 1 means that the diurnal modes only are to be taken. Imposing the additional requirement that the derivatives with respect to of the semi-diurnal

components vanish and again making use of the properties of the Fourier components of velocity at the poles as given by (8) and (9) it is seen that the four expressions for the convective derivative are reduced to two expressions. All other terms of the Navier-Stokes equations, i. e. the driving forces, drag forces, Coriolis forces etc. are also vectors in the horizontal shell given by r = constant. For this reason the same kinematical conditions expressed by (8) and (9) hold for all the terms of (4). Thus, from these considerations it is seen that at each pole the four Navier-Stokes equations that remain (two for each of the diurnal modes and velocity components) are really only two independent equations. The over-determination of the problem at the poles is therefore only apparent and not real. By using the procedure outlined above we have guaranteed that our solutions will satisfy the Navier-Stokes equations at the poles and will be continuous over the whole globe.

Although the vertical velocity does not appear in our set of equations, it should be remarked that the behaviour of the Fourier components of the vertical velocity at the poles is completely different. All the modes of the vertical velocity except the average (or zero) mode vanish identically at the poles.

The Iteration Procedure

The problem has now been reduced to a system of non-linear algebraic equations where for each mesh point in latitude and altitude there are ten unknowns and ten equations. If latitude differences of five degrees and altitude differences of 20 km are chosen then for the altitude range of 120 km to 500 km

there result 7400 equations with 7400 unknowns. These are reduced by our boundary conditions at 120 km to 7030 unknowns. These equations are represented symbolically by

$$\mathbf{F}(\mathbf{V}) = \mathbf{R} \tag{14}$$

where $\mathbf{F}$ represents a non-linear matrix operator on the 7030 unknowns represented by the vector $\mathbf{V}$. The vector $\mathbf{R}$ on the right hand side of (14) is derived from the pressure gradients and also has 7030 components. The method adopted to solve the above system of equations is a double iteration scheme consisting of a single Newton-Ralphson procedure combined with a Gauss-Seidel iteration (Ortega and Rheinboldt, p. 214). To apply the Newton-Ralphson technique we expand about a previous iterative value $\mathbf{V}^{(i)}$, where for $i = 0$ we use some initial estimate (usually zero). This may be expressed as

$$\mathbf{F}(\mathbf{V}^{(i)}) + \frac{\partial \mathbf{F}(\mathbf{V}^{(i)})}{\partial \mathbf{V}_j} (\mathbf{V}^{(i+1)} - \mathbf{V}^{(i)}) = \mathbf{R} \tag{15}$$

or

$$\frac{\partial \mathbf{F}(\mathbf{V}^{(i)})}{\partial \mathbf{V}_j} (\mathbf{V}^{(i+1)} - \mathbf{V}^{(i)}) = \mathbf{R} - \mathbf{F}(\mathbf{V}^{(i)}) \tag{16}$$

where $\partial \mathbf{F}/\partial \mathbf{V}_j$ is the Jacobian $\mathbf{J}$ or Frechet derivative. We shall denote $\mathbf{V}^{(i+1)} - \mathbf{V}^{(i)}$ by $\mathbf{W}^{(i+1)}$. Equation (16) results in the formal solution

$$\mathbf{V}^{(i+1)} = \mathbf{V}^{(i)} + \mathbf{J}^{-1}(\mathbf{R} - \mathbf{F}(\mathbf{V}^{(i)})) \tag{17}$$

or

$$W^{(i+1)} = J^{-1} (R - F(V^{(i)})) \tag{18}$$

Obviously the direct inversion of the matrix J or the solution by an elimination process is not possible with the present computational facilities. To obtain a solution a double iteration scheme is required.

To accomplish this we may order the vector V and the Jacobian J in either of two ways. The first method (hereafter referred to as method one) is illustrated in figures 1 to 4. The matrix J is ordered into blocks where each block corresponds to a certain altitude. The blocks themselves are ordered into sub-blocks according to latitude. These sub-blocks are matrices of order 10×10 according to the ten Fourier modes of the velocities. With this ordering the Jacobian Matrix has the form of a tri-diagonal block form matrix in which the non-linear terms appear only in the diagonal block. A Gauss-Seidel iteration procedure is adopted, in which the matrix J is decomposed as follows

$$J = D - L - U \tag{19}$$

where D, L, U are the diagonal, the lower tri-angular and upper tri-angular matrices respectively. The matrices L and U in this case contain terms arising only from the viscous coupling in the vertical direction. Let the index k denote a fixed altitude and D_k, L_k and U_k the sub-blocks of D, L and U corresponding to the index k. Then the system of equations (16) can be written as

$$D_k (V_k^{(i)}) W_k^{(i+1)} = L_k W_{k-1}^{(i+1)} + U_k W_{k+1}^{(i)} + (R - F(V^{(i-1)}))_k \tag{20}$$

with k running from one to nineteen.

The matrices L_k and U_k have diagonal block form. Equation (20) represents a system of 370 non-homogeneous linear algebraic equations. The right hand side is known explicitly. Due to the tri-diagonal form of D_k the solution can be obtained by a tri-diagonal block elimination scheme (Varga, 1962, p. 196).

The matrices D_k, L_k and U_k are computed from algebraic expressions. These algebraic expressions are obtained by differentiating the system of non-linear algebraic difference equations with respect to the unknowns, i.e. the components of V. The construction of these expressions, as well as the formation of the algebraic equations themselves, was performed with the aid of Formac (Sammet, 1967), a computor program which performs algebraic manipulations.

An alternate scheme (method 2) is to order the vector V and the Jacobian matrix according to 37 blocks of latitude. Each of the blocks of size 190×190 is ordered according to altitude. Thus the index k in equation (20) denotes a fixed latitude. In this scheme the matrices L_k and U_k contain terms arising from the non-linearities of the Navier Stokes equations. The matrix D_k is again of tri-diagonal block form and the solution can be obtained by tri-diagonal block elimination as described above. An advantage of this method (method 2) is that with an initial value of zero for the velocities of the start of the iteration scheme the velocities obtained from the first iteration are the solutions of the Navier-Stokes equations when the non-linear and horizontal viscosity terms are ignored. This linear solution will contain the full effects of vertical viscosity. Thus it corresponds to the results of previous investigations (Geisler, 1967; Bailey et al, 1968).

The first method of ordering converged in all cases independent of mesh size, though it required a large number of iterations. The second method of ordering did not converge in all cases studied. Both methods yielded the same solution when convergence was obtained. The second method was applied to mesh sizes of five and ten degrees in latitude. Convergence was obtained at equinox conditions for a ten degree mesh without difficulty. To obtain convergence for the five degree mesh at equinox conditions a convergence factor (Ortega, 1970, p. 187) was added to the diagonal elements of the Jacobian. Convergence was obtained at solstice with a ten degree mesh in latitude also, by adding a convergence factor to the Jacobian. No convergence was obtained at solstice conditions with a five degree mesh in the second method, although various weight factors and smoothing techniques were attempted. Also the Jacobian method of iteration (Ortega, 1970) was attempted in this case with no better success.

The second method of ordering was used to test the accuracy with respect to changes of the altitude mesh size and to study the effects of various ion drag and viscosity coefficients.

2. ANALYSIS OF FORCES

The Driving Force

The right hand side of our system of equations (4) are the driving forces $\vec{f}_d$ that arise from the horizontal pressure gradients. The driving force is given by

$$\vec{f}_d = -\frac{1}{\rho} \nabla_h P \tag{21}$$

We may derive $\vec{f}_d$ from a given atmospheric model that specifies the density and temperature distribution as a function of latitude, local time τ and height z. In the lower thermosphere the driving forces are relatively small and therefore the geostrophic approximation of the equations of motion given by

$$2 [\vec{\omega} \times \vec{V}] = -\frac{1}{\rho} \nabla_h P \tag{22}$$

yields fairly accurate results for the wind field. The winds are controlled by the Coriolis force and are perpendicular to the pressure gradients as is apparent from equation (22). In the thermosphere this is not true as we may no longer neglect the other terms of the equation of motion, especially the inertial terms. The winds that result from an integration of the equation of horizontal motion are in a direction that is close to the direction of the pressure gradients, as will be shown by our results and also by previous work on this subject. For this reason the global pattern of the pressure gradients is the most important parameter in the determination of the thermospheric global wind pattern. We shall specify some of the characteristics of the pressure gradients used in our computation.

Similar to most previous calculations (Geisler, 1967, Kohl and King, 1967) we have chosen the Jacchia model for the determination of the pressure gradients as this model yields a density distribution that is in close agreement with satellite drag derived densities in the isothermal region. The forces are derived by a differentiation process from the quantities described by the atmospheric model, therefore the reliability of the forces so derived will be considerable less than that of the density and the temperature given by the model. In particular we would like to point out the uncertainties that arise when the Jacchia model is used.

(1) In the Jacchia model the density ρ and temperature T are continuous functions of the independent variables θ, τ and z. This is equally true for the poles. On the other hand the derivatives of density and temperature are not continuous at the poles and therefore the driving force remains undefined at the poles. For a global description of the driving forces it is therefore necessary to modify the Jacchia model in the polar regions. We have used such a modification (Blum and Harris, 1973) to overcome this difficulty.

(2) The temperature in the Jacchia model is a model parameter and not necessarily identical with the true kinetic temperature. For this reason the pressure calculated from Jacchia's model may deviate from the true pressure both in amplitude and in phase. If incoherent back scatter radar observations of temperatures are used in place of the Jacchia model temperatures, it may be expected that a more realistic pressure pattern would be obtained. Such a

pressure pattern would introduce a phase shift in the wind pattern of approximately half the phase difference between radar temperature and drag derived densities.

(3) At present the data on the density and temperature distribution are inadequate to form a definite global model in the height region between 120 to 250 km. Therefore the pressure gradients deduced from the Jacchia model for this height region are extremely unreliable and no great validity should be attached to the computed wind pattern below 250 km. The effect of this uncertainty of the driving force and with it the flow pattern, on the isothermal region is not very considerable. The reason for this is that the coupling between the flow patterns at various heights is only through the viscosity term $\eta \partial^2 v / \partial z^2$. This term is not very important in the lower thermosphere as the kinematic viscosity has a relatively low value in this height region. Due to its exponential increase with height it only becomes important at higher altitudes (Figure 12). The influence of the flow below 250 km on the flow on the isothermal region will therefore be small. The pattern in the isothermal region is essentially determined by the forces that exist in this height region and not by the flow at lower altitudes.

(4) Relatively minor modifications of the density and temperature distribution especially as regards their latitudinal dependence which is less well known that their local time dependence, may have considerable effect on the meridional driving force and thereby on the meridional flow pattern. Drag data do not

permit a determination of the latitudinal variations of the atmosphere that is sufficiently accurate to conclusively ascertain the meridional pressure gradients. A slightly different model of the latitudinal density dependence would result in a substantially altered meridional force. The wind pattern, especially the meridional winds, that would result from the pressure gradients based on the densities determined from the OGO 6 mass spectroscopic observations (Hedin et al. 1972) would be different in essentials from the winds derived with the driving forces based on Jacchia's model.

We shall describe some of the properties of the driving forces that result from Jacchia's model:

(1) At equinoxes the Jacchia model is symmetric with respect to the equator. For this reason both amplitudes and phases of the azimuthal driving forces are equal for the corresponding points of the two hemispheres. The meridional forces for corresponding points are equal in amplitudes but have a phase difference of 12 hours, i.e. the forces at corresponding points are both directed either towards the equator or the respective pole. Furthermore, the diurnally averaged meridional force (i.e. the Fourier component of order zero) is directed towards the equator for both hemispheres. It has a maximum amplitude at a latitude between 40° and 30°. This result differs from Rishbeth's result (1972) who has determined a vanishing diurnal average meridional force from the Jacchia model. On the other hand the amplitude of the diurnal variation of the meridional force is always larger than the diurnally averaged component as shown by figure 5 for the northern hemisphere.

(2) At summer solstice the diurnally averaged meridional forces are directed towards the south pole for all latitudes. They have a maximum near a latitude of 30°. At winter solstice the direction is reversed and the maximum of the force is at -30°. In contrast to equinox conditions the amplitude of the diurnal variation of the meridional forces is less than the diurnal average amplitude in the latitude region between 30° to -20° for summer solstice conditions. Therefore the meridional forces in this latitude belt point during the whole diurnal cycle to the south in summer and north in winter. Figure 6 shows this behaviour of the driving forces at summer solstice conditions.

(3) In the Jacchia model the shape of the local time variation of the pressure and especially its extrema, are independent of latitude. From this follows immediately that all Fourier components of the azimuthal and meridional driving forces are 90° out of phase.

(4) We shall investigate the dependence of the driving forces on height and solar activity. It will be seen that in the isothermal region a first approximation yields driving forces that increase almost linearly with height and are nearly independent of solar activity. These properties of the driving forces can easily be demonstrated by numerical computations based on the Jacchia model. With respect to the linear height dependence this is shown in figures 5 and 6. Analytically these properties become apparent when the slight dependence of the driving forces on the variation of the mean molecular weight M with latitude and local time is neglected. In order to show the dependence of the driving forces on the separate variations of temperature and density we may rewrite equation (21)

$$\vec{f}_d = -\frac{1}{\rho}\nabla_h P = -\frac{RT}{M}\nabla_h \ln\rho - \frac{R}{M}\nabla_h T + \frac{RT}{M^2}\nabla_h M \tag{23}$$

$$\vec{f}_d = -gH\nabla_h \ln P = -gH\nabla_h \left(\ln P_0 - \int_{z_0}^{z} dz/H\right) \tag{24}$$

with H the mean scale height and R the universal gas constant.

Using (24) as our starting point we note that in the Jacchia model the pressure P at the lower boundary does not depend on geographical position, local time and solar activity. Therefore

$$\vec{f}_d = gH \int_{z_0}^{z} \frac{\partial}{\partial x}\left(\frac{1}{H}\right) dz \tag{25}$$

where we have replaced ∇_h by $\partial/\partial x$ for convenience of notation and x is any horizontal coordinate. The forces for to a single atmospheric constituent become

$$\vec{f}_d = gT \int_{z_0}^{z} \frac{\partial}{\partial x}\left(\frac{1}{T}\right) dz = gT \frac{\partial}{\partial x}\int_{z_0}^{z} \frac{dz}{T} \tag{26}$$

The variations of the temperature T are derived from the Jacchia model

$$T(z, x) = T_\infty(x) - (T_\infty(x) - T_{120}) \exp(-\sigma(z - z_0)) \tag{27}$$

where σ is related to the temperature gradient at the lower boundary and is only slightly dependent on T_∞, the exospheric temperature. T_∞ itself is dependent on x (local time and latitude) and on the solar activity S

$$T_\infty(S, x) = T_0 (1 + \alpha S)\, r(x) \tag{28}$$

where $\alpha = 3.24$ (flux units)$^{-1}$ and not depending on either x or S, $T_0 = 383°$ an extrapolated value of the exospheric temperature for S = 0 and r(x) describes the dependence of the exospheric temperature on latitude and local time. As will be seen in the following, the near independence of the driving forces on solar activity is due to the possibility to express the exospheric temperature by eq. (28) where the function r is independent of S. Equations (27) and (28) make it possible to evaluate the integral $\int_{z_0}^{z} dz/T$ in closed form with the result

$$\int_{z_0}^{z} dz/T = (z - z_0)/T_\infty (S, x) + \ln \left(\frac{T(z, x)}{T_{120}}\right) \Big/ (T_\infty (S, x)\sigma) \qquad (29)$$

The force $\vec{f}_d$ becomes for the isothermal region, where T is replaced by T_∞,

$$\vec{f}_d = - gz/T_\infty \cdot \frac{\partial T_\infty}{\partial x} + g T_\infty/\sigma \cdot \frac{\partial}{\partial x} \left(\ln \left(\frac{T_\infty}{T_{120}}\right) \Big/ T_\infty\right) \qquad (30)$$

The second term of (30) is independent of the height z. The linear dependence of the forces on altitudes results immediately from (30) with the coefficient $-g/T_\infty \, \partial T_\infty/\partial x$. The variation of the forces with solar activity is given by

$$\partial \vec{f}_d/\partial S = g z \, \frac{\partial}{\partial S} \frac{\partial}{\partial x} (\ln T_\infty) - g/\sigma \, \frac{\partial}{\partial S} T_\infty \frac{\partial}{\partial x} (\ln (T_\infty/T_{120})/T_\infty) \qquad (31)$$

The first term of (31) vanishes due to the form of T_∞ according to (28). The second term must be calculated explicitly:

$$\frac{\partial}{\partial S} T_\infty \frac{\partial}{\partial x} \left(\ln \left(\frac{T_\infty}{T_{120}} \right) \Big/ T_\infty \right) = \frac{\partial}{\partial S} \frac{\partial}{\partial x} \left(\ln \left(\frac{T_\infty}{T_{120}} \right) \right) - \frac{\partial}{\partial S} \left(\ln \left(\frac{T_\infty}{T_{120}} \right) \frac{\partial T_\infty}{\partial x} \Big/ T_\infty \right) \qquad (32)$$

The first term of (32) vanishes again because it is a mixed derivative of $\ln T_\infty$. A further evaluation of the second term of (32) yields the final result

$$\partial \vec{f}_d / \partial S = \frac{g}{\sigma} \frac{r'}{r} \frac{\alpha}{1 + \alpha S} \qquad (33)$$

In order to evaluate the relative change of $\vec{f}_d$ with solar activity we use the simple estimate

$$| f_d | = g z \left| \frac{r'}{r} \right| \qquad (34)$$

derived from (26) and therefore

$$\frac{1}{| f_d |} \left| \frac{\partial f_d}{\partial S} \right| = \frac{1}{\sigma z} \frac{\alpha}{1 + \alpha S} \qquad (35)$$

For the determination of the relative change of $\vec{f}_d$ given by (35) we have to use the constants of the Jacchia model ($\sigma \approx 0.03\ \mathrm{km}^{-1}$). For a solar activity S = 200 and a height z = 300 km we obtain

$$\frac{1}{| f_d |} \left| \frac{\partial f_d}{\partial S} \right| \approx \frac{1}{1800} \qquad (36)$$

A change of 50 flux units would therefore cause only a fractional change of the forces of about 3% which is insignificant. While our derivation is not strictly

correct for the real atmosphere which has several constituents, it is a good approximation for the isothermal region because there the driving forces are mainly due to the variations of atomic oxygen which is the major constituent in the isothermal region below 500 km. The exact numerical computation for the dependence of the forces on solar activity bears out the above estimates: below 250 km the dependence of the driving force on solar activity is complicated and no clear trend is easily discernable, above 250 km the near independence of the driving force on solar activity is reaffirmed by the numerical results.

The local time and latitudinal distribution of the driving force at a height of 300 km is shown for both equinox and solstice conditions in figures 7 and 8.

The Ion Drag Force

The ion drag force $\vec{f}_{ion}$ per unit mass is given by

$$\vec{f}_{ion} = \nu_{in} (\vec{V}_{ion} - \vec{V}) \frac{N_i}{N} \tag{37}$$

where $\vec{V}_{ion}$ is the ion velocity and ν_{in} the ion-neutral collision frequency for momentum transfer. The collision frequency is proportional to the density and depends slightly on the types of ions present (Stubbe, 1968). The drag force is therefore determined by the ion velocity and the ion distribution. We have not used the individual distributions for each ion species for the determination of $\vec{f}_{ion}$, but used the approximate expression (Chapman, 1965) that gives the ion-neutral collision frequency as a function of N the total density. This expression is

$$\nu_{in}/N = 2.6 \times 10^{-9}/\sqrt{M} \text{ sec}^{-1} \text{ cm}^3 \tag{38}$$

where N is the neutral number density and M the average molecular weight. An alternate approximation of the ion drag force (Dalgarno, 1964) follows from the relation

$$\nu_{in}/N = 7.3 \times 10^{-10} (T/1000)^{0.4} \tag{39}$$

Expression (39) yields slightly different results for the ion drag force. A more elaborate procedure for the evaluation of ν_{in} is possible, but not necessary as the uncertainties of the ion density distribution determine the accuracy.

In the height region where the collision frequency ν_{in} is larger than the ion gyro frequency the ion velocity will be close to the neutral velocity and the ion drag force will be negligible. This is the case for altitudes below 150 km.

In the height region where the ion gyro frequency is much larger than the collision frequency ν_{in} the ions are constrained by the electromagnetic forces. There exists a transition region between 150 km to 200 km where the ion motion is controlled partially by the neutral motion and partially by the electromagnetic forces. In this region the drag forces are difficult to estimate (Lindzen, 1967), although the relative low ion densities in this height region tend to decrease the importance of the ion drag force in the equations of motion.

Thus in addition to the uncertainties of the pressure gradients in the lower thermosphere the uncertainty of the ion drag force will contribute to the unreliability of the computed wind field in the lower thermosphere.

It has been inferred that electric fields in the ionosphere exist due to the Sq current distribution. Generally the electric fields will be perpendicular to the geomagnetic field and the ion motion perpendicular to the geomagnetic field will be given by

$$\vec{V}_{ion\perp} = \vec{E} \times \vec{B}/B^2 \tag{40}$$

The ion motion parallel to the geomagnetic field is determined by the neutral motion and given by

$$\vec{V}_{ion\parallel} = (\vec{V}_N \cdot \vec{B})\vec{B}/B^2 \tag{41}$$

where $\vec{V}_N$ is the neutral air velocity. In the absence of electric fields the ion drag force does not depend on the magnitude of $\vec{B}$, but only on the direction of $\vec{B}$. Assuming electric fields do exist and are well-known, then the inclusion of the ion drag due to the ion velocity normal to $\vec{B}$ in our equations of motion does not pose any problem. The term $[ExB]/B^2$ does not involve the neutral velocities and one could therefore just add the ion drag due to the electric fields to the right hand side of the equations, i.e. to the pressure gradients.

Electric fields in the ionosphere are difficult to observe directly, so that the information about them comes from theoretical deductions of ionospheric behaviour. Commonly the electric field of the E-region is extrapolated to higher altitudes. From Maeda's (1971) analysis a lunar component and a solar component of the electric potential coexist. Both are of the same order of

magnitude but for the steady state wind field only the solar component is required. Following Maeda we have calculated the ion velocities normal to $\vec{B}$ and have found them to depend strongly on the higher harmonics of Maeda's analysis. For instance if only the P_1^1 with $1 \leq 2$ are included then ion velocities of less than 10 m/sec result. If P_1^1 with $1 \leq 4$ are included the ion velocities would become as large as 57 m/sec. Inclusion of even high terms of the harmonic representation of the electric potentials would probably result in entirely different, and probably larger ion velocities, as the amplitudes of the higher spherical harmonics in the representation of the electric potentials do not fall rapidly enough to compensate the effects of differentiation. For this reason the ion velocities normal to $\vec{B}$ in the height region of interest to us are not well known. Generally (Rishbeth, 1972) it is assumed that they are less than 30 m/sec. In the region where the neutral winds are mainly determined by the amplitude of the ion drag force, a first approximation of the effect of the ion motion normal to $\vec{B}$ will be simply the addition of the ion velocity to the wind velocity. This is seen from the linearized equations of motion. Thus, while the ion motion normal to $\vec{B}$ may be important for particular aspects of the global wind field, like the diurnal average zonal motion, i.e. the superrotation of the atmosphere, they are not very significant for the general global flow pattern. From these consideration, especially the uncertainty of the electric fields themselves, we have decided not to include the electric fields in our wind computations. With the above assumptions the ion drag force $\vec{f}_{ion}$ becomes

$$f_{ion}^{(\theta)} = 2.6 \times 10^{-9} N_i V^{(\theta)}/\sqrt{M} \cdot \cos^2\theta/(1 - 0.75 \sin^2\theta) \qquad (42)$$

$$f_{ion}^{(\phi)} = 2.6 \times 10^{-9} N_i V^{(\phi)}/\sqrt{M}$$

By dividing the equations of motion (1.4) by ω we may define a dimensionless ion drag coefficient

$$D_{ion} = 2.6 \times 10^{-9} N_i/(\sqrt{M} \cdot \omega). \qquad (43)$$

The horizontal component of the magnetic field $\vec{B}$ deviates from the meridional direction by the declination angle D. D depends both on longitude and latitude. If the dependence of D on longitude is taken into account, then the ion drag forces become dependent on universal time. We cannot include in our treatment the variations of D without raising the number of independent variables from 3 to 4 and abandoning the steady state approach. We have therefore to assume that the earth's magnetic dipole is alligned with the earth's axis. This simplification, equivalent to setting D = 0 causes the meridional ion drag force to vanish at the equator. As a result of the reduced drag in the equatorial zones rather high meridional velocities and velocity gradients result from the computation, especially at solstice conditions. This is obvious for the linearized equations of motion, which become extremely simple at the equator as the Coriolis force also vanishes. The non-linear equations avoid this difficulty, but even then the meridional velocity gradients are large and the convergence process is slow or the iteration scheme may even diverge. Without making assumptions contrary to

physical realities we may avoid this difficulty by noting that the meridional ion drag depends only on the absolute value of the angle between the magnetic field lines and the meridian. We may take the average value of this angle at the equator as 11.3°, as a magnetic dipole tilted by 11.3° gives the best fit to the geomagnetic field (Mead, 1970). The latitude Φ_m which corresponds to a magnetic inclination I of 11.3° is 5.8°. In line with this reasoning we have substituted at all latitudes Φ with $|\Phi| \leq 5.8°$ in the expression for the meridional ion drag given by (42) instead of the factor $\cos^2\theta/(1-0.75\ \sin^2\theta)$ the value of that factor at a latitude of 5.8°. This value is 0.0384. Due to this substitution the meridional ion drag force does not vanish at the equator and we have avoided difficulties in the convergence process.

In order to complete the global representation of the ion drag force it is necessary to know the ion density as a function of height, latitude and local time, day of the year and solar activity. It will be a challenge for theorist in the future to construct a three dimensional model where the ion density is calculated consistently with the neutral density and the wind system. In our computation we have not attempted such a consistent treatment but used a given model of ion distribution to determine the drag force. In a early stage of a our computation an approximate distribution was used, but in the final calculation we have used the Penn State Ionospheric Model which gives numerical values for the ion densities as a function of all the above mentioned parameters. In addition, the ion density in the Penn State model is dependent on the geographic longitude λ.

This is not in line with our steady state picture that does not allow functional dependence on the longitude alone, but only on the local time $\lambda - \omega t$. In order to adept the Penn State model for our purposes we have averaged the ion densities over all longitudes and used these average densities in order to determine the drag force. In the actual computation the Fourier coefficients up to second order of this longitudinal averaged drag force where used. In this process the longitudinal averaging reduced the semi-diurnal component of the drag force relative to the average drag force to a considerable degree when a comparison was made with the drag force that referred to a given fixed longitude. The diurnal component of the longitudinal-averaged drag force was also reduced, but somewhat less than the semi-diurnal component. The diurnal average of the ion drag coefficient is represented in figures 9 and 10 for a solar activity of $\overline{F}_{10.7} = 200$ at both equinox and solstice conditions. Figure 11 shows also the time dependent components of the ion drag for equinox at the equator. The above mentioned figures show that the ion drag coefficient, even after our longitudinal averaging, is not entirely symmetric at equinoxes. Also the winter and summer solstice coefficients are not exactly anti-symmetric with respect to the equator. The causes of these deviations from symmetry are the various geographical and seasonal anomalies of the ion distribution. For these reasons the computed winds will also have slight deviations from the symmetry that would be expected from the symmetric pressure gradients.

The Viscous Forces

The viscous forces in the equations of motion are given by

$$\vec{f}_{vis} = \mu/\rho \cdot \left(\nabla^2 \vec{V} + \frac{1}{3} \nabla(\nabla \cdot \vec{V})\right) \tag{44}$$

where μ is the dynamic viscosity coefficient and $\eta = \mu/\rho$ the kinematic viscosity. The term $1/3\ \nabla(\nabla \cdot \vec{V})$ is small, it vanishes completely for a constant density flow. In neglecting it and also dropping $\partial V^{(r)}/\partial\theta$ and $\partial V^{(r)}/\partial\phi$ we obtain for the viscous forces in the azimuthal and the meridional direction in spherical coordinates (Eskinazi, p. 206):

$$f_{vis}^{(\phi)} = \eta \left(\nabla^2 V^{(\phi)} - \frac{V^{(\phi)}}{r^2 \sin^2\theta} + \frac{2\cos\theta}{r^2 \sin^2\theta} \frac{\partial V^{(\theta)}}{\partial\phi}\right) \tag{45}$$

$$f_{vis}^{(\theta)} = \eta \left(\nabla^2 V^{(\theta)} - \frac{V^{(\theta)}}{r^2 \sin^2\theta} - \frac{2\cos\theta}{r^2 \sin^2\theta} \frac{\partial V^{(\phi)}}{\partial\theta}\right) \tag{46}$$

After writing the differential operator explicitly (Eskinazi, p. 207) we may resolve the horizontal viscous force into two parts: vertical viscosity which is associated with vertical velocity shears, and horizontal viscosity which is associated with horizontal velocity shears.

The vertical viscosity is approximately equal to the expression $\eta\,\partial^2 V/\partial z^2$ which is usually used in an approximate treatment of the equations of motion. In our treatment we have included the horizontal viscosity as well (except at the poles where it is negligible small). It is given by the expressions

$$\frac{1}{\eta} f_{vis}^{(\theta)} = \frac{1}{r^2 \sin\theta} \frac{\partial}{\partial\theta} \left(\sin\theta \frac{\partial V^{(\theta)}}{\partial\theta} \right) + \frac{1}{r^2 \sin^2\theta} \frac{\partial^2 V^{(\theta)}}{\partial\theta^2} - \frac{V^{(\theta)}}{r^2 \sin^2\theta} - \frac{2\cos\theta}{r^2 \sin^2\theta} \frac{\partial V^{(\phi)}}{\partial\phi} \quad (47)$$

$$\frac{1}{\eta} f_{vis}^{(\phi)} = \frac{1}{r^2 \sin\theta} \frac{\partial}{\partial\theta} \left(\sin\theta \frac{\partial V^{(\phi)}}{\partial\theta} \right) + \frac{1}{r^2 \sin^2\theta} \frac{\partial^2 V^{(\phi)}}{\partial\phi^2} - \frac{V^{(\phi)}}{r^2 \sin^2\theta} + \frac{2\cos\theta}{r^2 \sin^2\theta} \frac{\partial V^{(\theta)}}{\partial\phi} \quad (48)$$

While the vertical viscosity terms are at all latitudes of great importance for the resulting flow pattern, the horizontal viscosity terms are only important when the meridional or azimuthal velocity gradients are large. Our results show that this is indeed the case in a band of latitudes near the equator. The order of magnitude of the horizontal viscosity terms becomes in this narrow latitude band almost as large as the main terms of the equation of motion. Furthermore the inclusion of the horizontal viscosity in the calculation facilities the convergence of the iteration process, because the horizontal velocity gradients are decreased by it and therefore the non-linear terms of the convective derivative of the velocity become smaller, thereby decreasing the influence of the nonlinearities and speeding up the convergence process.

The kinematic viscosity increases exponentially with altitude because the density decreases exponentially. Generally an approximation for the viscosity is used (Rishbeth, 1972). In our calculations a somewhat more accurate method was applied: The dynamic viscosity coefficient as a function of temperature for the various atmospheric constituents was taken from the results of Yun et al. (1962) and then the Jacchia model was used to calculate the appropriate temperature and composition at the latitude, altitude and local time in question.

For each altitude and latitude the value of the kinematic viscosity was Fourier-analysed and the resulting Fourier coefficients up to second order used in the computations. The exact expression for the dynamic viscosity coefficient we used was

$$\mu = \Sigma\, \mu_{0i} \left(\frac{T - 273.2}{1000}\right)^{\alpha_i} n_i/N \qquad (49)$$

where the summation was for molecular nitrogen, molecular oxygen and atomic oxygen. n_i are the respective number densities, N the total number density and the μ_{0i} and α_i are

$$\mu_{0i} = 4.017.10^{-4},\ 4.771.10^{-4},\ 4.771.10^{-4}$$

$$\alpha_i = 0.62,\ 0.59,\ 0.59 \qquad i = 1 \text{ to } 3$$

The dependence of the kinematic viscosity in the atmosphere on height is shown in figure 12 both for the diurnal average value of the viscosity and for the time-dependent components. It is seen that the ratio of the diurnal component to the diurnal average increases with height from a value zero at 120 km to about 20% at 500 kilometers. This shows the importance of including a diurnal variation of the viscosity in the isothermal region. The time of the maximum of the viscosity also changes considerably from the lower thermosphere, where it is in phase with the temperature, to the isothermal region where it has a phase difference of 12 hours relative to the maximum of density. In the upper thermosphere the diurnal variation of density becomes more important than the diurnal

variation of temperature for the evaluation of the kinematic viscosity which is approximately proportional to $T^{0.6}/\rho$.

Boundary Conditions

(a) Lower Boundary

Little is known about the steady state diurnal variation of the atmosphere in the 120 km height region. For this reason no observationally founded assumption regarding the lower boundary conditions for the global thermospheric wind field can be made. The pressure gradients are probably very small in this region, but so are the viscous and drag forces. For these reasons a steady state wind velocity of the order of 100 m/sec at 120 km cannot be discounted. In our computation we have assumed no winds at 120 km in line with the Jacchia model used by us. Fortunately the effect of a possible wind field at 120 km on the global wind pattern above 180 km is negligible, as the coupling between adjacent height layers is only through the viscosity term of the equation of motion. The kinematic viscosity coefficient at 120 km is almost 5 orders of magnitude less than at 500 km (Figure 12), thereby decreasing the coupling to a very considerable degree. We performed a test calculation with a non-vanishing wind field at 120 km. No,or only very little change in the resulting wind fields above 160 km were noted as will be shown in Part 2. This result is also in accordance with the result of Lindzen (1967).

(b) Upper Boundary

The upper boundary conditions are derived generally from considerations involving the viscous forces. It is easy to see (Rishbeth, 1972) that $\partial^2 V/\partial r^2 \rightarrow 0$

at exospheric heights is required in order to balance the equations of motion. The generally accepted deduction that this implies also $\partial V/\partial r \rightarrow 0$ is not as well established by strict theoretical considerations. Nevertheless we have also used in our calculations the condition $\partial V/\partial r \rightarrow 0$. In a discussion whether boundary conditions with $\partial \vec{V}/\partial r \neq 0$ are possible it would be necessary to analyse the transition region between the collision controlled height region and the collision free region above the exosbase.

Chapman and Cowling (1952) have discussed the behaviour of the viscosity coefficient at low gas densities and have found it to be decreasing under certain conditions, but no strict treatment of the transition region at the exosbase regarding the horizontal wind shears is known to the authors, so that a possibility of $\partial V/\partial r \neq 0$ cannot be entirely discounted. In this respect it may be remembered that King-Hele (1971) has observed the average azimuthal velocity of the atmosphere to be decreasing above 300 km to at least 500 km. Obviously these observations cannot be reconciled with a boundary condition $\partial V/\partial r = 0$, so that observational evidence does also not decisively confirm the assumption $\partial V/\partial r = 0$ that is generally made.

In part 2 the resulting wind field will be discussed.

Acknowledgement

We express our gratitude to Professor John Nisbet of the State University of Pennsylvania Ionospheric Research Laboratory who put the computer program of the Penn State Mark I Ionospheric Model at our disposition.

REFERENCES

Bailey, G. J., R. J. Moffet and H. Risbeth, Solution of the coupled ion and neutral air equations of the mid-latitude ionospheric F2 layer, J. Atmos. Terr. Phys., 31, 253-270, 1969.

Blum, W. P., Harris, I., Empirical Models of the Upper Atmosphere in the Polar Regions, to be published in Planet and Space Sci., 1973.

Challinor, R. A., Neutral air winds in the ionosphere F-region for a symmetric global pressure system, Planet. Space Sci., 18, 1485-1487, 1970.

Chapman, S., The electrical conductivity of the ionosphere, Nuovo Cim. 4, 1385-1412, 1965.

Chapman, S., Cowling, T. S., The Mathematical Theory at Non-Uniform Gases, Cambridge Press, London, 1960.

Cho, H. R. and K. C. Yeh, Neutral winds and the behavior of the ionpsheric F2 region, Radio Science, 5, 881-894, 1970.

Dalgarno, A. Ambipolar diffusion in the F region, Jr. Atmos. Terr. Physics, 26, 939, 1964.

Eskinazi, S., Vector Mechanics of Fluids and Magnetofluids, Academic Press, New York, N. Y., 1967.

Geisler, J. E., A numerical study of the wind system in the middle thermosphere, J. Atmos. Terr. Phys., 29, 1469-1482, 1967.

Hedin, A. E., Mayr, H. G., Reber, A., Carignan, G. R., Spence, N. W., Cospar Conference, Madrid, 1972.

Jacchia, L. G., Static diffusion models of the upper atmosphere with empirical temperature models, Smithsonian Contr. to Astrophys., 8, #9, 215-257, 1965.

Jacchia, L. G., Revised static models of the thermosphere and exosphere with empirical temperature profiles, Smithsonian Astrophysical Observatory Special Report 332, 1971.

Kallina, Carl, "Periodicity and Stability for Linear and Quasi-Linear Parabolic equations SIAM J. Appl. Math., 18, 601-618 (1970).

King-Hele, D. G., Decrease in upper atmosphere rotation rate at heights above 350 km, Nature 233, 325-326, 1971.

Kohl, H., King, J. W., Atmospheric Winds between 100 and 700 km and their effects on the ionosphere, Journal of Atmos. Terr. Physics 29, 1045-1062, 1967.

Lindzen, R. S., Reconsideration of Diurnal Velocity Oscillation in the Thermosphere, Journal of Geoph. Res. 22, 1591-1598, 1967.

Lindzen, R. S., Internal gravity waves in atmospheres with realistic dissipation and temperature. Part I. Mathematical development and propagation of waves in the thermosphere, Geophys. Fluid Dynamics, 1, 303-355, 1970.

Lindzen, R. S., Chapman, S., Atmosphere Tides, Space Sci. Rev. 10, 1-188, 1969.

Maeda, H., Solar and Lunar Hydromagnetic Tides in the Earth Magnetosphere, Journal of Atmos. Terr. Physics, 33, 1135-1146, 1971.

Mead, G. D., International geomagnetic reference field 1965.0 in dipole coordinates, Journal Geophys. Res. 75, 4372-4374, 1970.

Nisbet, J. S., On the construction and use of the Penn State MK I ionospheric model, Ionospheric Research Scientific Report No. 355, 1970.

Ortega, J. M., Rheinboldt, W. C., "Iterative Solution of Non-Linear Equations in Several Variables," Academic Press, New York, N.Y., (1970).

Risbeth, H., Thermospheric Winds and F-region: A Review, Journal of Atmos. Terr. Physics 34, 1-47, 1972.

Rüster, R., Dudeney, J. R., "The importance of the non-linear term in the Equation of motion of the Neutral Atmosphere," Journal of Atm. and Terr. Physics, 34, pp. 1075-1083. (1972).

Sammet, J., "Formula Manipulation by Computer," Advances in Computers, 8, Academic Press, New York, N.Y., pp. 47-102, (1967).

Stubbe, P., Frictional forces and collision frequencies between moving ion and neutral gases, Jr. Atmosph. Terr. Physics, 30, 1965-1985, 1968.

Varga, Richards, "Matrix Iterative Analysis," Prentice-Hall, Inc., Englewood, Cliffs, N. Y., (1962).

Volland, H., Mayr, H. G., A Theory of the diurnal variations of the thermosphere, Ann. Geophys. 26, 907-919, 1970.

Volland, H., Mayr, H. G., A Three Dimensional Model of Thermosphere Dynamics, 34, Jr. of Atmosph. and Terr. Physics, 1745-1768, 1972.

Yun, K. S., Weissman, E., Mason, E. A., High temperature transport properties of dissociating nitrogen and dissociating oxygen, 5, The Physics of Fluids, 672-678, 1962.

FIGURE CAPTIONS

Figure 1. Structure of Jacobian Matrix $J = \partial F/\partial V_j$ according to iteration method 1 (basic Newton-Rapphson iteration scheme for one altitude layer superimposed Gauss-Seidel iteration over altitude range). For iteration method 2 structure would be similar, but there would be 37 blocks of 190 rows. Each block would correspond to one latitude. Matrix J is tri-diagonal, all elements not in blocks indicated are zero. For these elements no computer storage is required. Sub-matrices type D_k: All elements of these matrices correspond to the same altitude. They arise from the various terms of the equations of motion. Some terms are also due to viscosity. Sub-matrices types L_k and U_k: These sub-matrices couple adjacent altitude layers by the viscosity term $\eta(\partial^2 V/\partial z^2)$. They are diagonal in the sense that all their sub-blocks of order 10×10 are on the diagonal. If viscosity would be neglected the matrices L_k and U_k would vanish. Sub-matrix D_{19}: This sub-matrix has a special structure due to upper boundary condition $\partial V/\partial z = 0$ at 500 km.

Figure 2. Fine structure of sub-matrices of type D_k shown in Figure 1. Matrices D_k have sub-blocks of order 10×10 denoted by DD_{ki}, DL_{ki} and DU_{ki}. Most of the elements of DD_{k1} and DD_{k37} are zero due to the polar boundary conditions. The elements of the matrix DD_{ki} are due to the main terms of the equation of motion. Some of them are also due to the non-linear terms of the convective derivative and the viscosity coupling. Matrices DL_{ki} and

DU_{ki} couple various latitudes at a fixed altitude. These sub-matrices would vanish when the non-linear terms of the convective derivative and the horizontal viscosity coupling are neglected.

Figure 3. Structure of sub-matrices L_k and U_k of Figure 1. The matrices L_k and U_k are diagonal in the sense that their sub-blocks, which themselves are matrices of order 10×10, are all on the diagonal. The reason for this diagonal structure is that viscosity coupling between adjacent altitude layers is only considered between mesh points of the same latitude. In method 2 the equivalent matrices would couple adjacent latitudes at the same altitude and would therefore not have this simple structure. Matrices LD_{k1} and LD_{k37} have special form due to boundary conditions at the poles. Matrices LD_{ki} couple adjacent height layers due to vertical viscosity. Coupling exists only when latitudes are equal. The sub-structure of LD_{ki} shows that BM couples the meridional flow and BZ the zonal flow. As the viscous drag does not couple meridional to zonal flow when the altitudes differ, the off-diagonal sub-blocks of LD_{ki} vanish.

Figure 4. Structure of matrices DL_{ki}, DD_{ki} and DU_{ki} of Figure 2. Computor storage for all the 300 elements detailed here is required. Matrices DDM, DDZ and DD1 have numbers as their elements. DDM, DDZ and DD1 are 5×5 matrices, DL is a 10×10 matrix. Matrices DD1 couple meridional to zonal velocities. Their elements are due to the Coriolis force, the non-linear elements of the convective derivative and the horizontal viscosity

terms. The off-diagonal elements of matrices DDM and DDZ couple the various Fourier modes. If a further linearization of the equations of motion is made (additional to the linearization of the convective derivative) and the products of higher Fourier modes are neglected then all off-diagonal elements of columns 2-5 and rows 2-5 would vanish and the various Fourier modes decouple, thus greatly simplifying the computations.

Figure 5. The height and latitude dependence of the driving force as deduced from Jacchia's model at equinox conditions with a solar activity $F_{10.7} = 200$. The diurnal average meridional force and the diurnal amplitudes of the azimuthal and meridional forces are shown. The diurnal average of the azimuthal force is zero, or nearly zero. The forces are shown for altitudes of 200, 300, 400 and 500 km. The Jacchia model was modified in the polar region in order to fulfill the boundary conditions.

Figure 6. The same forces as shown in figure 5 for summer solstice conditions.

Figure 7. The global pattern of the driving force at a height of 300 km for equinox conditions.

Figure 8. The global pattern of the driving forces for summer solstice conditions.

Figure 9. The latitude dependence of the dimensionless diurnally averaged ion drag coefficient for equinox conditions and a solar activity of $F_{10.7} = 200$. The coefficients are represented for the altitudes 140, 220, 300, 380 and 460 km. Ion densities are deduced from the Penn State ionospheric model.

Figure 10. The latitude dependence of the diurnally averaged ion drag coefficients for summer solstice conditions and a solar activity of $F_{10.7} = 200$.

Figure 11. The height dependence of the average and time-dependent Fourier coefficients of the ion drag at equinox conditions and a solar activity of $F_{10.7} = 200$.

Figure 12. The height dependence of the diurnal average and time-dependent Fourier coefficients of the kinematic viscosity for equinox conditions at the equator as deduced from Jacchia's model at a solar activity of $F_{10.7} = 200$.

STRUCTURE OF MATRIX J (STAGE 1)

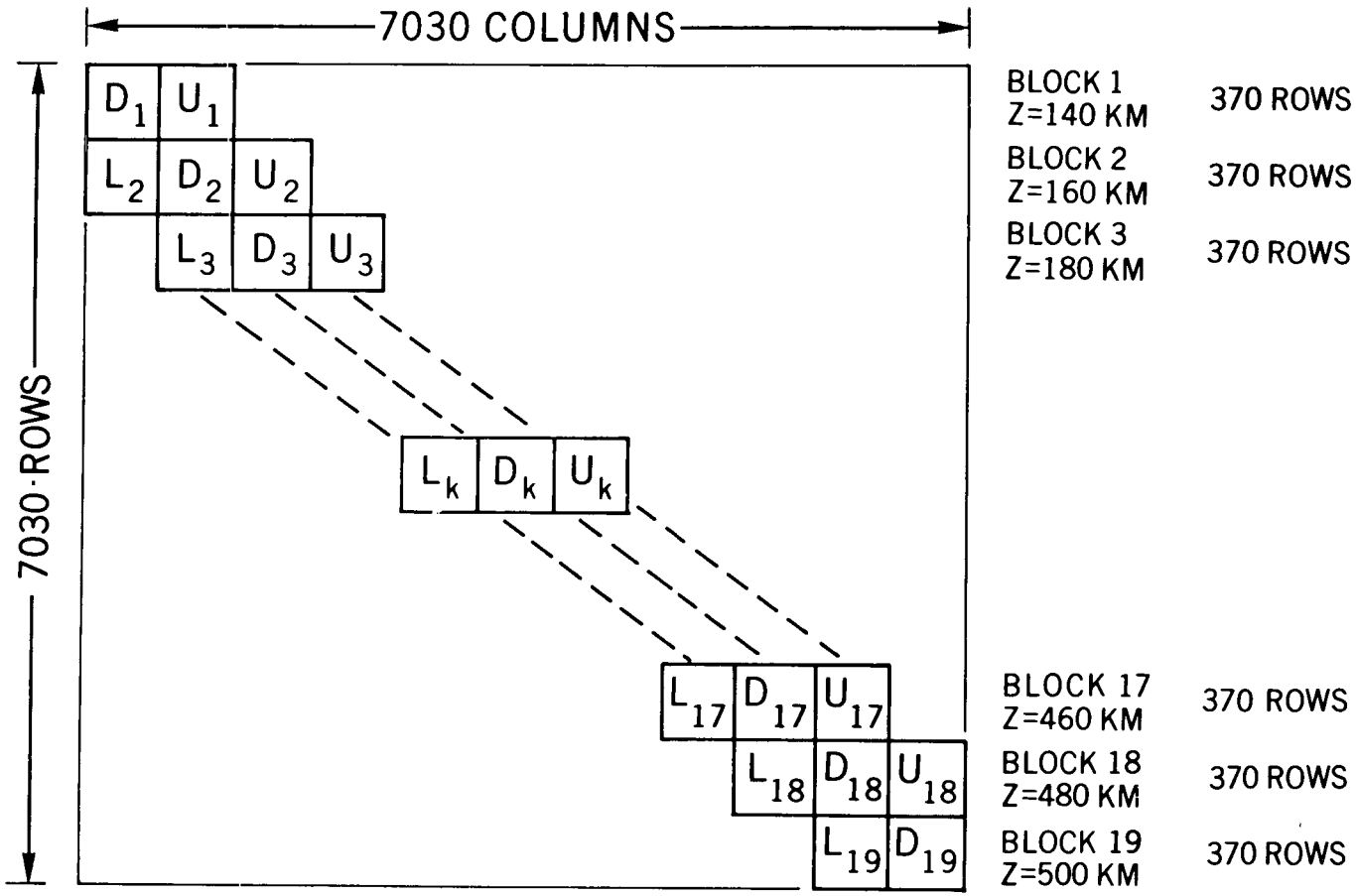

7030 ROWS IN 19 BLOCKS OF 370 ROWS EACH.
EACH BLOCK CORRESPONDS TO ONE ALTITUDE IN THE MESH

Figure 1

STRUCTURE OF MATRIX (STAGE 2)

FINE STRUCTURE OF MATRIX D_k

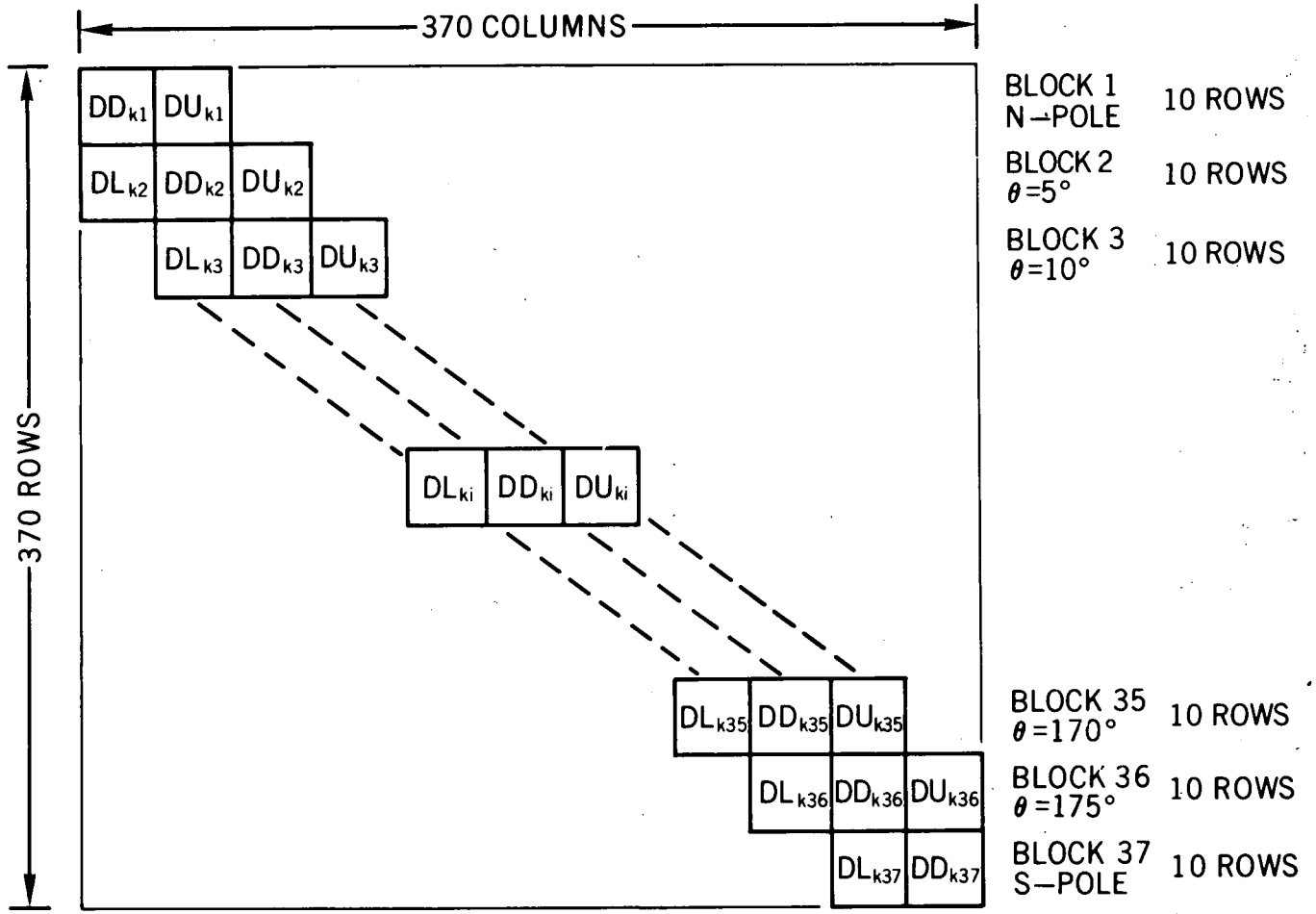

370 ROWS IN 37 BLOCKS OF 10 ROWS EACH. ALL MESHPOINTS REFER TO SAME ALTITUDE. EACH BLOCK CORRESPONDS TO ONE LATITUDE IN THE MESH.

Figure 2

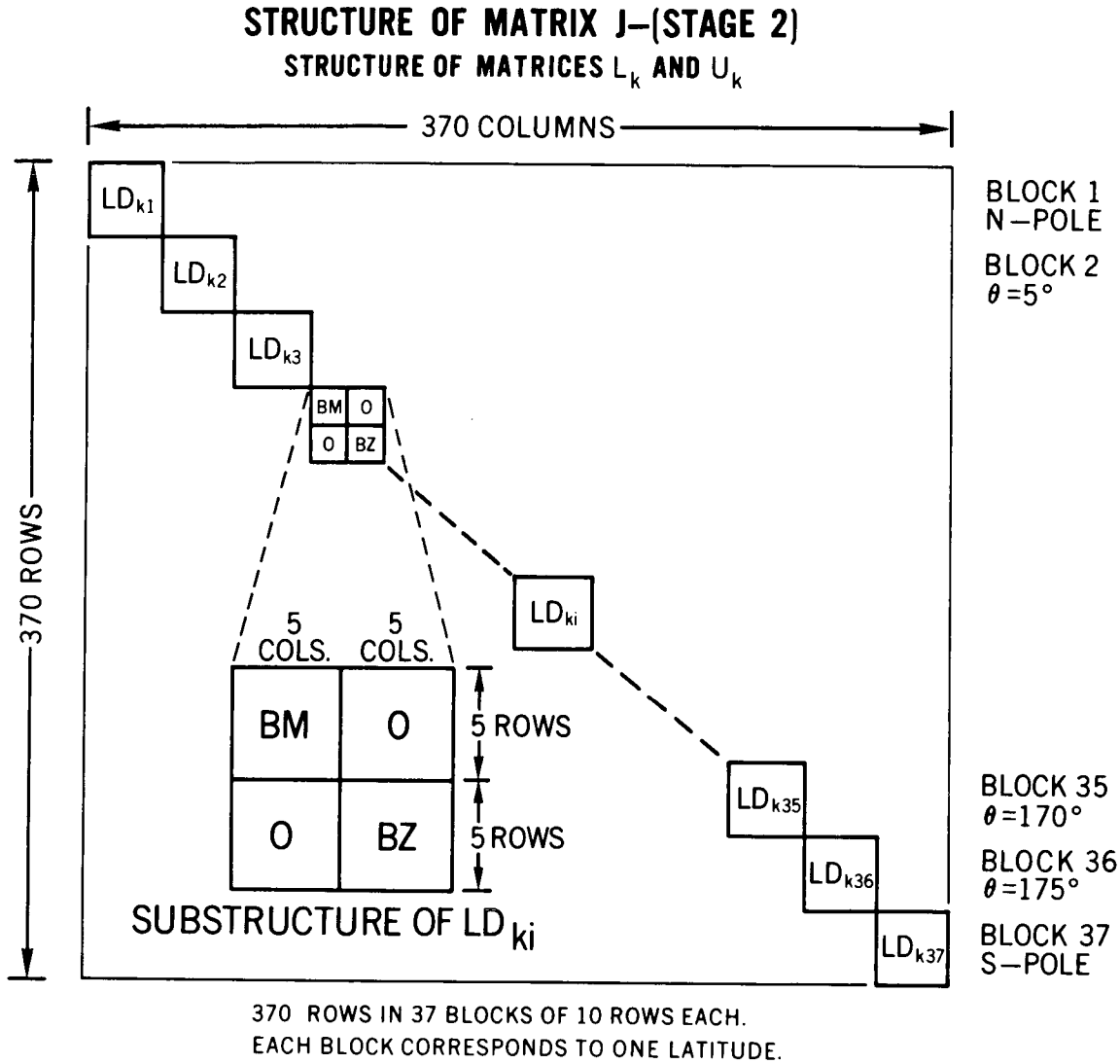
STRUCTURE OF MATRIX J–(STAGE 2)
STRUCTURE OF MATRICES L_k AND U_k
370 COLUMNS
370 ROWS
LD_{k1}
LD_{k2}
LD_{k3}
BM
O
O
BZ
LD_{ki}
5 COLS.
5 COLS.
BM
O
O
BZ
5 ROWS
5 ROWS
SUBSTRUCTURE OF LD_{ki}
LD_{k35}
LD_{k36}
LD_{k37}
BLOCK 1
N–POLE
BLOCK 2
θ=5°
BLOCK 35
θ=170°
BLOCK 36
θ=175°
BLOCK 37
S–POLE
370 ROWS IN 37 BLOCKS OF 10 ROWS EACH.
EACH BLOCK CORRESPONDS TO ONE LATITUDE.

Figure 3

STRUCTURE OF MATRIX J (STAGE 3)

FINE STRUCTURE OF MATRIX DD_{ki}

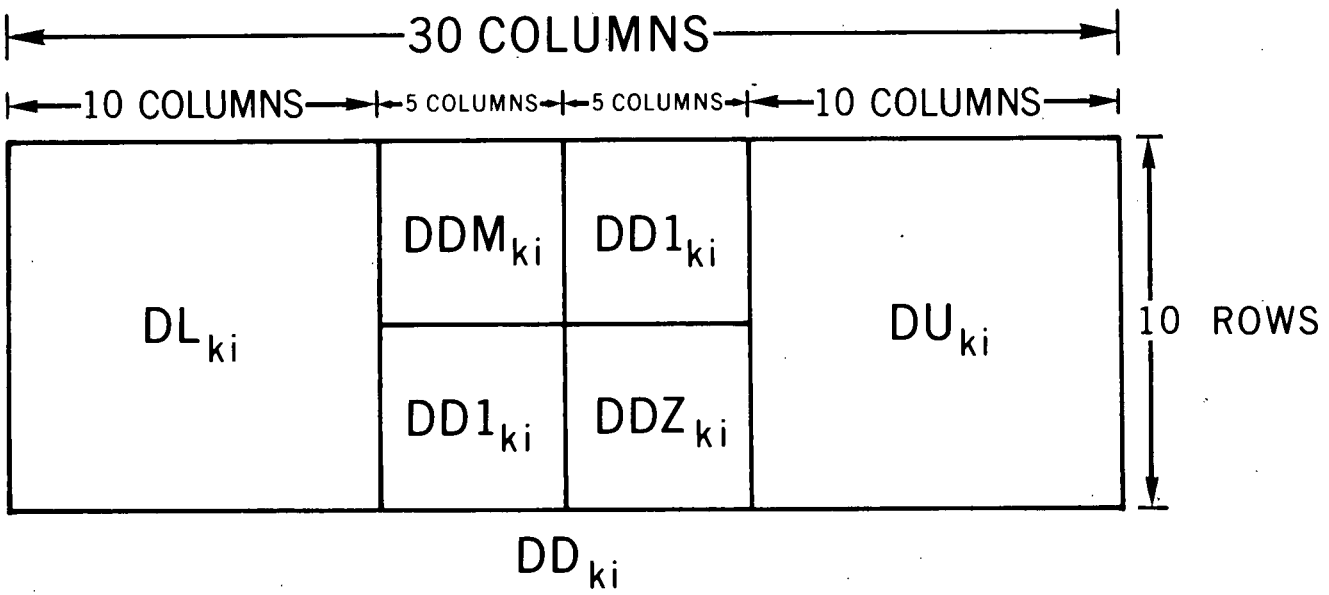

2 BLOCKS OF 5 ROWS EACH. ONE BLOCK CORRESPONDS TO MERIDIONAL VELOCITY, OTHER TO ZONAL VELOCITY

ALL TERMS OF MATRIX CORRESPOND TO SAME MESH POINT

Figure 4

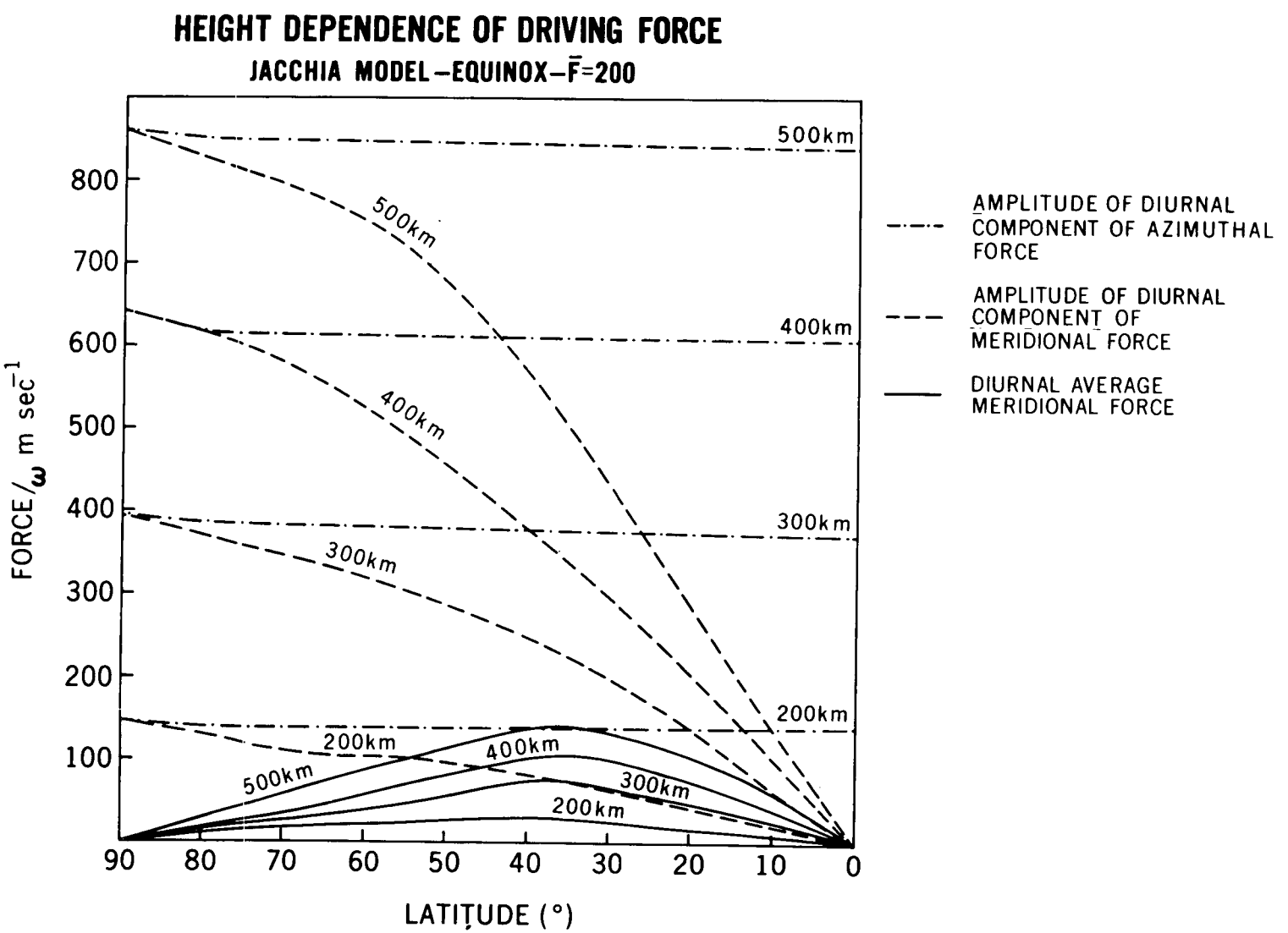
HEIGHT DEPENDENCE OF DRIVING FORCE
JACCHIA MODEL–EQUINOX–$\bar{F}$=200
FORCE/ω m sec^{-1}
LATITUDE (°)
800
700
600
500
400
300
200
100
90
80
70
60
50
40
30
20
10
0
500km
400km
300km
200km
AMPLITUDE OF DIURNAL COMPONENT OF AZIMUTHAL FORCE
AMPLITUDE OF DIURNAL COMPONENT OF MERIDIONAL FORCE
DIURNAL AVERAGE MERIDIONAL FORCE

Figure 5

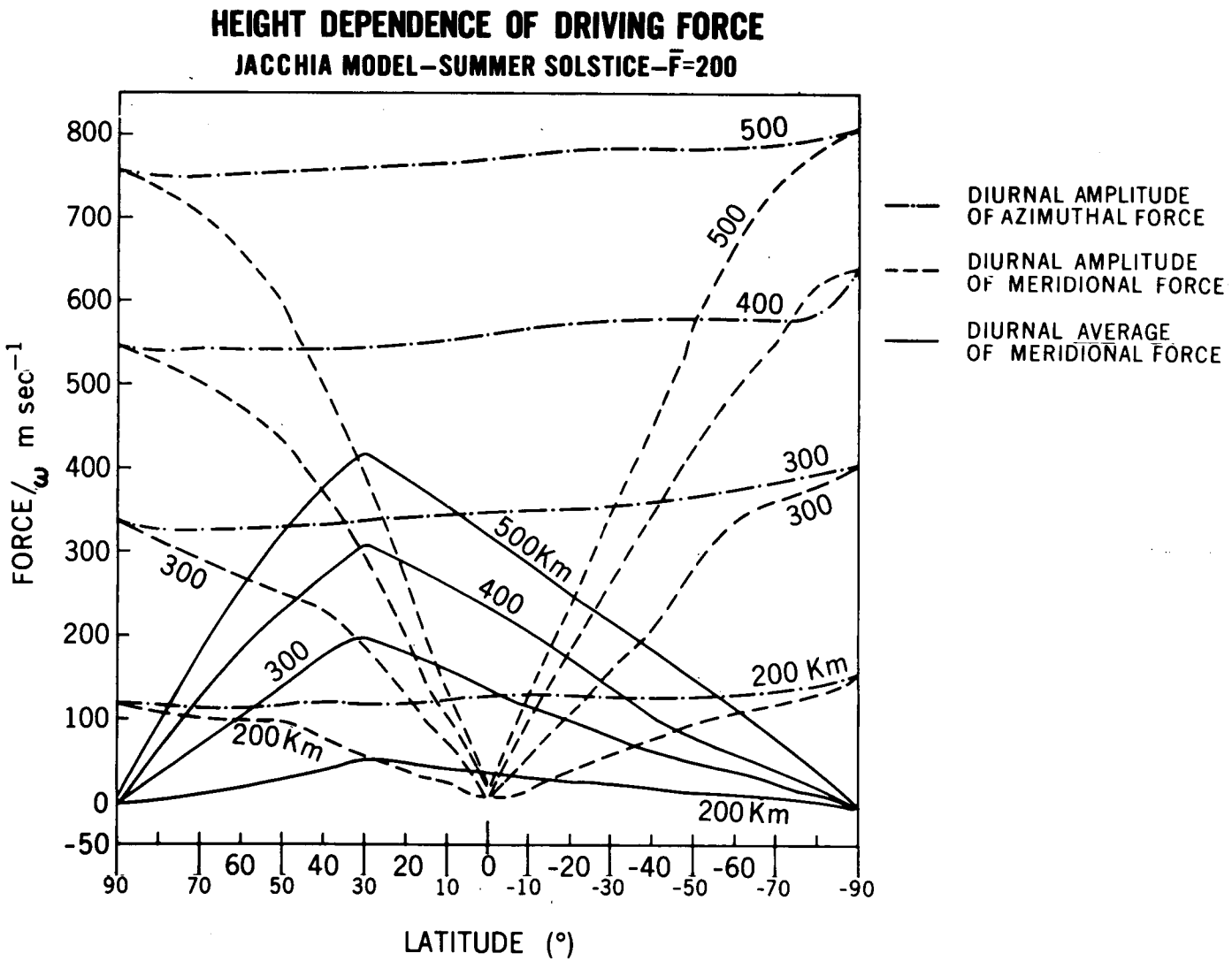
HEIGHT DEPENDENCE OF DRIVING FORCE
JACCHIA MODEL–SUMMER SOLSTICE–$\bar{F}$=200
FORCE/ω m sec^{-1}
800
700
600
500
400
300
200
100
0
-50
500
500
400
300
300
500Km
400
300
200 Km
200Km
200Km
90
70
60
50
40
30
20
10
0
-10
-20
-30
-40
-50
-60
-70
-90
LATITUDE (°)
DIURNAL AMPLITUDE OF AZIMUTHAL FORCE
DIURNAL AMPLITUDE OF MERIDIONAL FORCE
DIURNAL AVERAGE OF MERIDIONAL FORCE

Figure 6

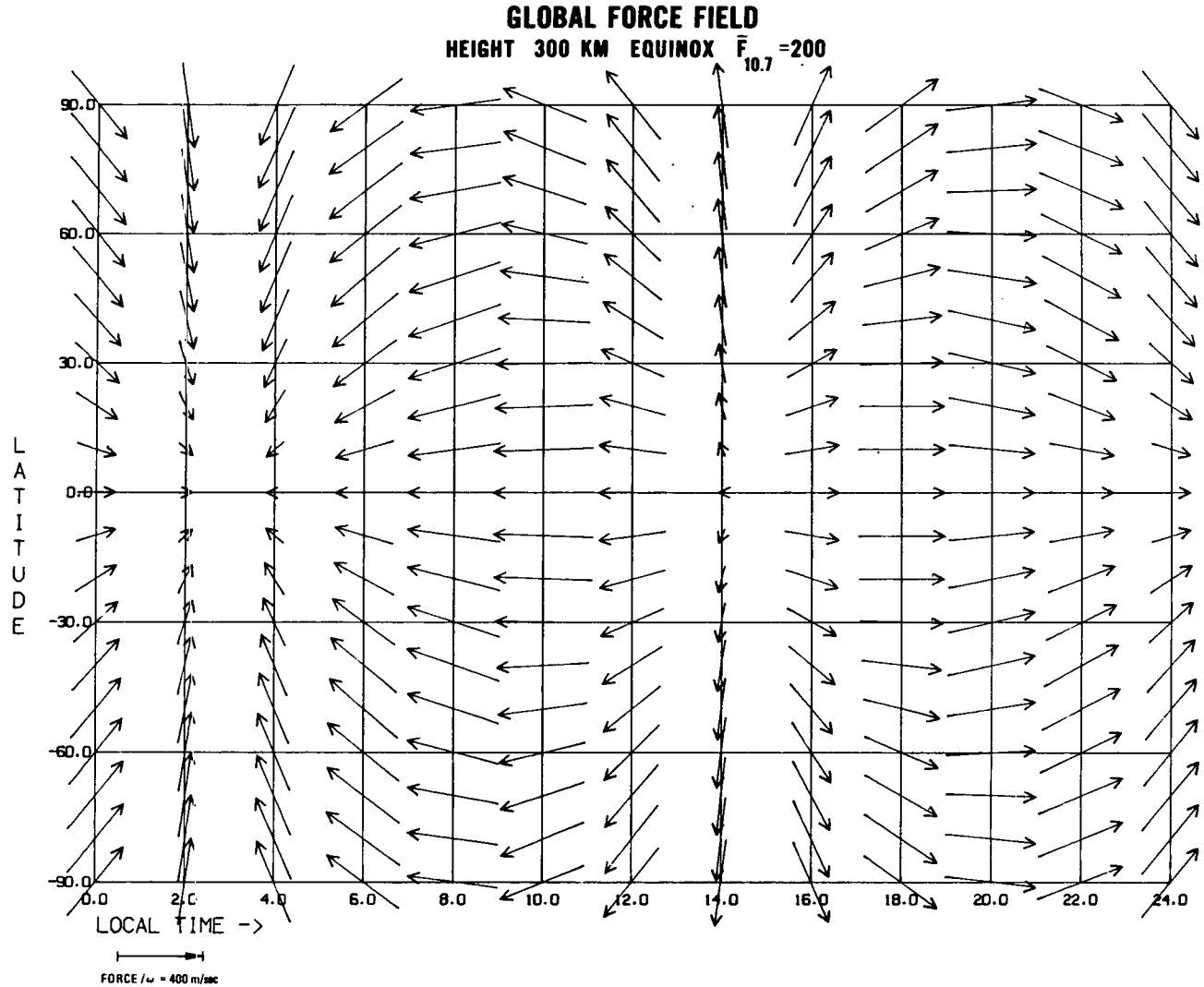
GLOBAL FORCE FIELD
HEIGHT 300 KM EQUINOX $\bar{F}_{10.7}$ =200
90.0
60.0
30.0
0.0
-30.0
-60.0
-90.0
LATITUDE
0.0
2.0
4.0
6.0
8.0
10.0
12.0
14.0
16.0
18.0
20.0
22.0
24.0
LOCAL TIME ->
FORCE/ω = 400 m/sec

Figure 7

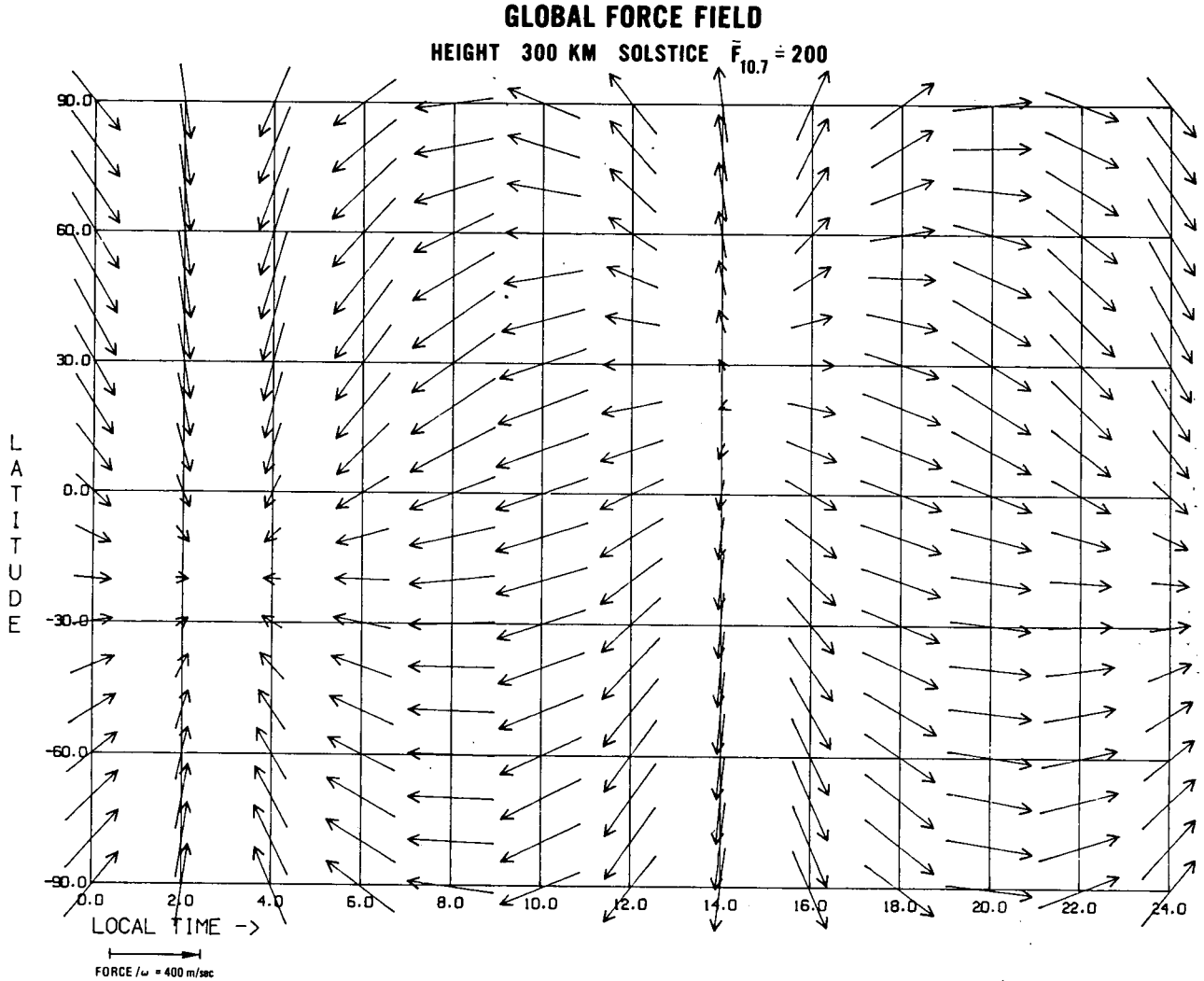
GLOBAL FORCE FIELD
HEIGHT 300 KM SOLSTICE $\bar{F}_{10.7} = 200$
90.0
60.0
30.0
0.0
-30.0
-60.0
-90.0
LATITUDE
0.0
2.0
4.0
6.0
8.0
10.0
12.0
14.0
16.0
18.0
20.0
22.0
24.0
LOCAL TIME ->
FORCE /ω = 400 m/sec

Figure 8

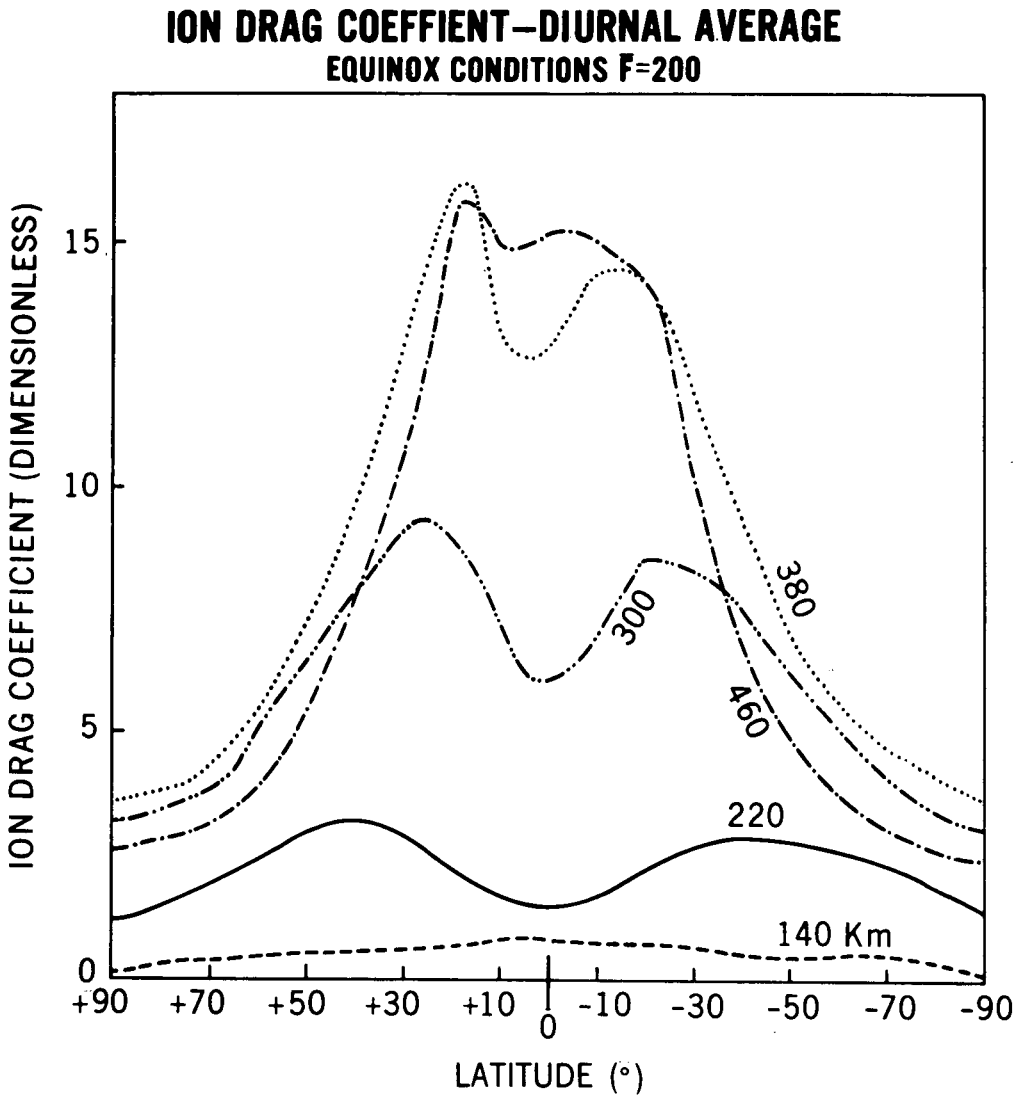
ION DRAG COEFFIENT–DIURNAL AVERAGE
EQUINOX CONDITIONS F=200
ION DRAG COEFFICIENT (DIMENSIONLESS)
15
10
5
0
380
300
460
220
140 Km
+90
+70
+50
+30
+10
0
-10
-30
-50
-70
-90
LATITUDE (°)

Figure 9

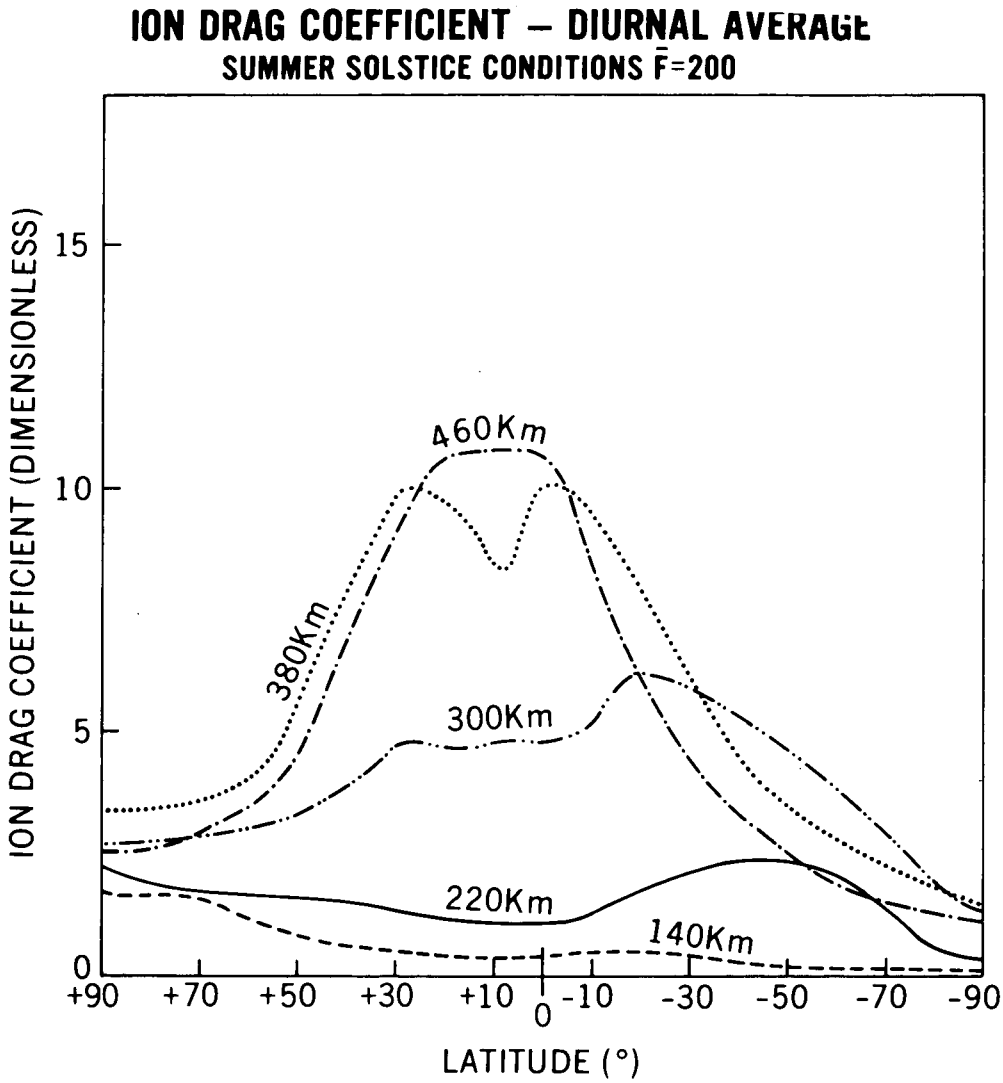
ION DRAG COEFFICIENT – DIURNAL AVERAGE
SUMMER SOLSTICE CONDITIONS F̄=200
ION DRAG COEFFICIENT (DIMENSIONLESS)
15
10
5
0
460Km
380Km
300Km
220Km
140Km
+90
+70
+50
+30
+10
0
-10
-30
-50
-70
-90
LATITUDE (°)

Figure 10

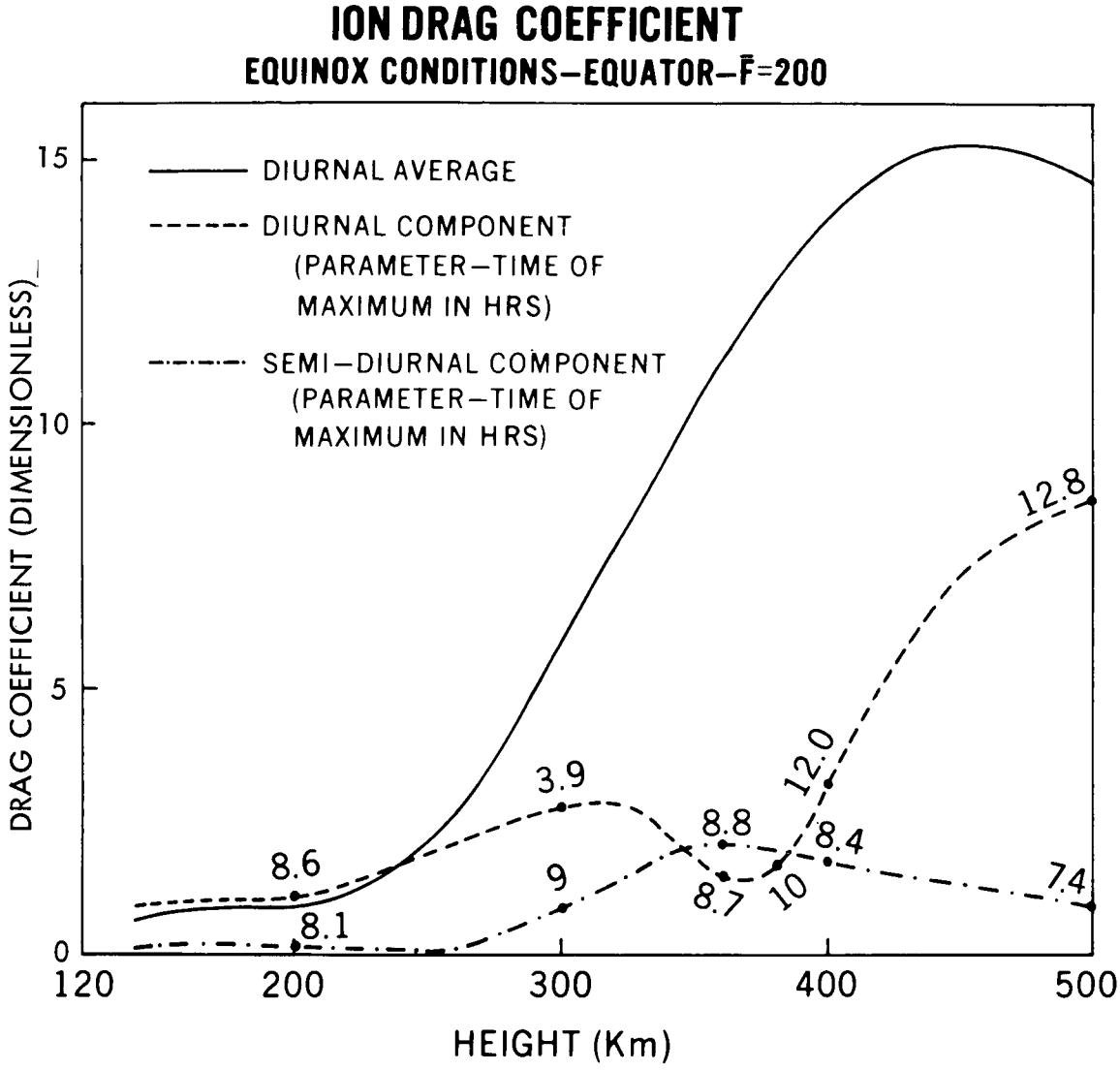
ION DRAG COEFFICIENT
EQUINOX CONDITIONS–EQUATOR–$\bar{F}$=200
DIURNAL AVERAGE
DIURNAL COMPONENT (PARAMETER–TIME OF MAXIMUM IN HRS)
SEMI–DIURNAL COMPONENT (PARAMETER–TIME OF MAXIMUM IN HRS)
DRAG COEFFICIENT (DIMENSIONLESS)
HEIGHT (Km)
0
5
10
15
120
200
300
400
500
8.6
3.9
8.8
12.0
12.8
8.1
9
8.7
10
8.4
7.4

Figure 11

KINEMATIC VISCOSITY
EQUINOX CONDITIONS - EQUATOR
$\bar{F}$=200

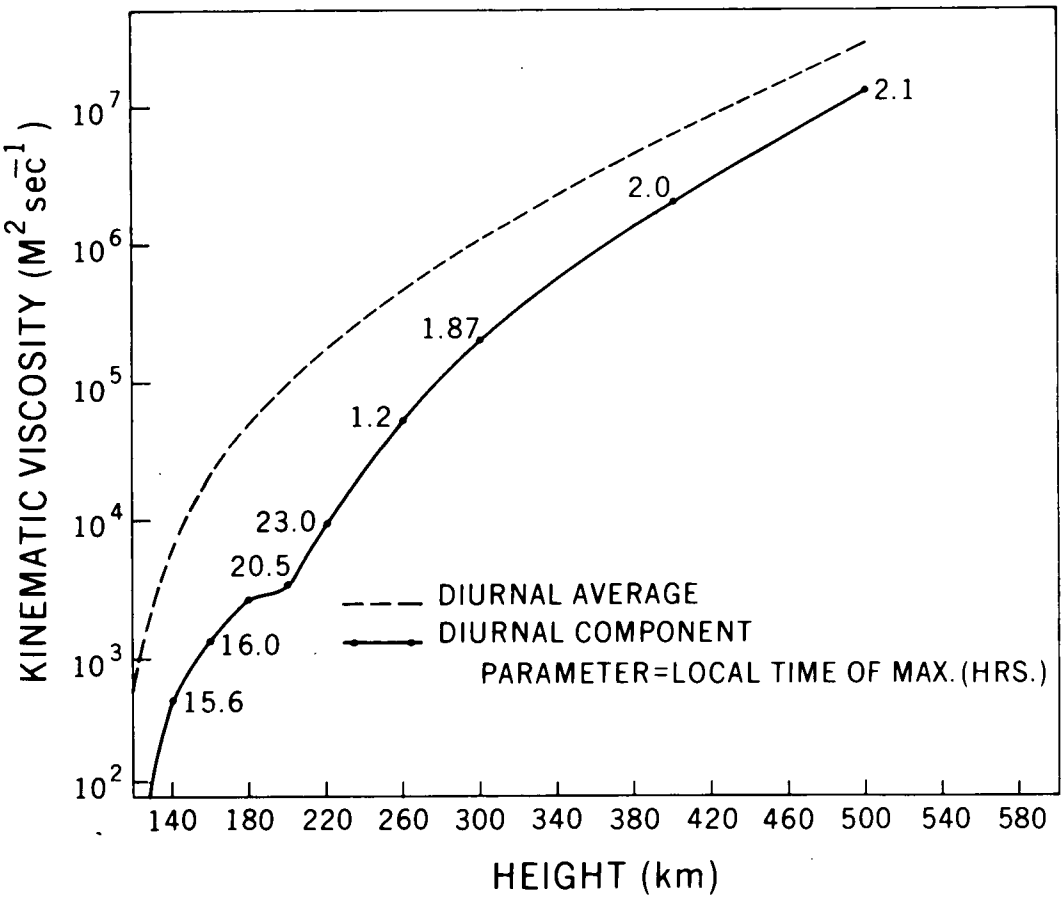

Figure 12

* U. S. GOVERNMENT PRINTING OFFICE: 1972—735-96